ELSEVIER

Polymer 41 (2000) 4965–4990

polymer

Investigation of the thermal curing chemistry of the phenylethynyl group using a model aryl ether imide

T.V. Holland, T.E. Glass, J.E. McGrath*

Department of Chemistry and NSF Science and Technology Center, Virginia Polytechnic Institute and State University, 2108 Hahn Hall, Blacksburg, VA 24061-0344, USA

Received 1 February 1999; received in revised form 13 July 1999; accepted 13 July 1999

Abstract

The high temperature curing reactions of oligomers bearing two phenylethynyl groups have previously been utilized to produce attractive new materials, but are not well understood. A model aryl ether imide compound with one such moiety was used to elucidate some of the chemistry occurring during these processes. It was demonstrated that oligomeric molecular weight soluble products were formed by thermal initiation at 375°C under nitrogen during these reactions, along with low molecular weight fragments derived from the model compound. These fragments were demonstrated to contain aliphatic protons in place of the phenylethynyl group and constitute about 5% of the overall material. Reactions of the model compound with deuterated biphenyl indicated that the reactive intermediates formed from the phenylethynyl moiety are able to abstract aromatic deuterium atoms in the presence of aromatic protons. However, these fragments appear to be side products not directly involved with the main curing reactions that occur after most of the carbon–carbon triple bonds have been reacted.

Keywords: 2-(Phenoxyphenyl)-5-(2-phenylethynyl)-1H-isoindole-1,3(2H)-dione; Nuclear magnetic resonance; High performance liquid chromatography

1. Introduction

The use of acetylene terminated reactive oligomers to produce networks upon thermal treatment (>200°C) has been known for more than 20 years [1,2]. More recently, terminal phenylethynyl groups have been used to produce tough, ductile, solvent resistant thermosets from low molecular weight oligomers by simple thermal initiation at higher temperatures (e.g. >350°C) [3–13]. These groups are particularly useful to prepare adhesives and polymer matrix composite materials because of a wide processing window between T_g and T_{cure} and since no volatiles are evolved during curing. The phenylethynyl moiety has been used as a pendant [1,8,9], internal [10] or reactive end group for polyimides [3–7], poly(arylene ether)s [2,11] and polybenzoxazoles [12–14]. The thermal curing of the phenylethynyl group at temperatures ranging from 350 to 400°C combines the properties of facile processing of the low molecular weight thermoplastic oligomers, with favorable solvent resistance and surprisingly ductile mechanical properties, for a thermoset. It appears possible that significant chain extension may occur prior to gel point [15]. Unfortunately, little is known about the mechanism of the curing reaction or the network structure and density.

A phenylethynyl model compound (I) was synthesized and has been used to study some aspects of the curing reaction. Some curing studies have been performed on ethynyl terminated oligomers designed to elucidate the curing mechanism [16–18]. Solid state NMR and IR of the intractable material indicated the presence of linear polymer, cyclotrimer and condensed polycyclic aromatics. Model compound studies containing only one ethynyl moiety per molecule produced soluble material and supported the conclusions derived from oligomer studies [19–21]. Much less study has been performed using the phenylethynyl moiety. Some model studies have been performed [3,4,22–24], but, few structures have been shown [24].

It was anticipated that the reaction products would be soluble and amenable to solution characterization. The structure was chosen to include only aromatic carbons and flexible aryl ether bonds which have also been mainly featured in previously studied polymer systems [4,5].

* Corresponding author. Tel.: +1-540-231-4457; fax: +1-540-231-8517.
E-mail address: jmcgrath@chemserver.chem.vt.edu (J.E. McGrath).

0032-3861/00/$ - see front matter
PII: S0032-3861(99)00578-9

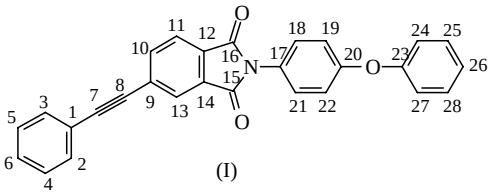

(I)

Scheme 1.

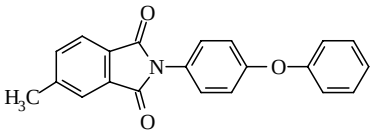

(II)

Scheme 2.

2. Experimental

2.1. General

4-Phenoxyaniline (4-POA) was purchased from the Aldrich Chemical Company and was recrystallized from water before use. The synthesis of 4-phenylethynylphthalic anhydride (4-PEPA) has been described previously [25]. It

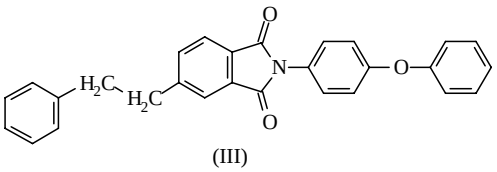

(III)

Scheme 3.

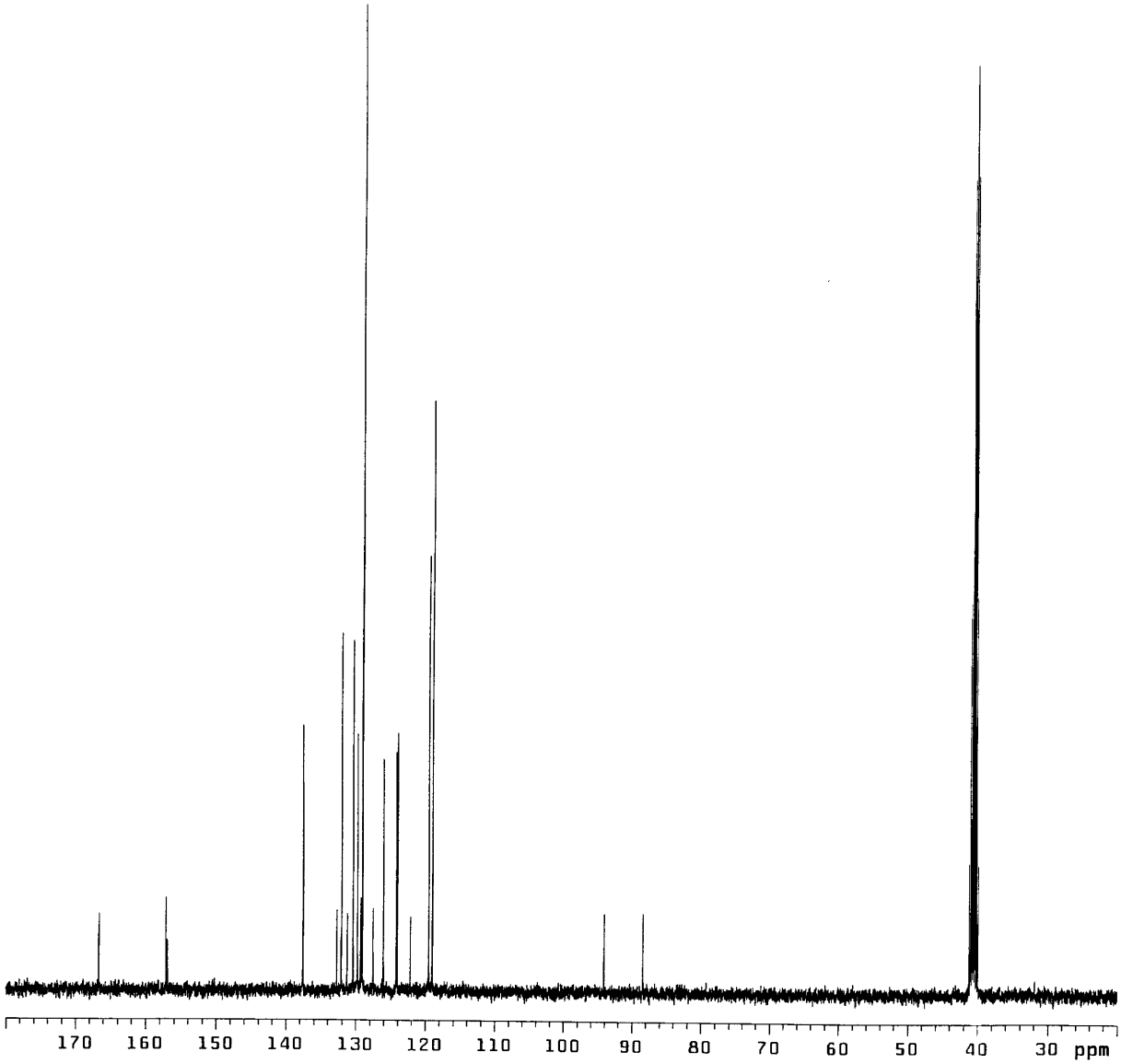

Fig. 1. ^{13}C NMR spectrum of model compound (I).

Table 1
Chemical shifts for carbon atoms in (I)

Carbon number	Chemical shift (ppm)
1	122.2
2	132.1
3	132.1
4	129.1
5	129.1
6	129.8
7	89.0
8	94.0
9	131.3
10	137.6
11	124.1
12	129.4
13	126.1
14	132.8
15	166.0
16	166.0
17	127.6
18	129.1
19	119.0
20	155.8
21	129.1
22	119.0
23	155.8
24	119.5
25	130.4
26	124.3
27	119.5
28	130.4

was purified by sublimation under vacuum at 165°C, then dried in a vacuum oven at 80°C overnight before use. 4-Methylphthalic anhydride (4-MPA) was purchased from Aldrich, purified by sublimation at 115°C and then dried in a vacuum oven at 50°C overnight. Diphenylacetylene

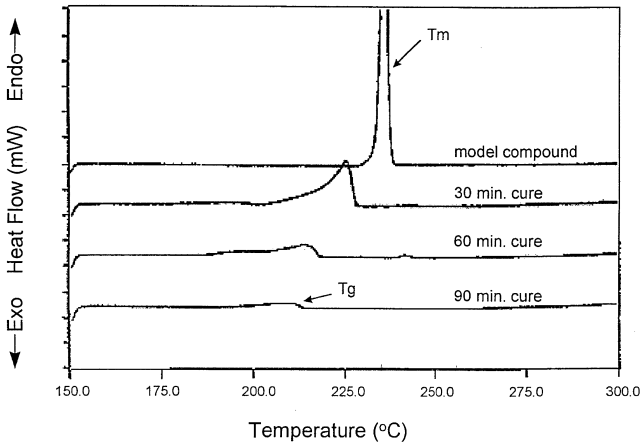

Fig. 3. DSC traces of (I) and cured samples.

(Aldrich Chemical Company) was purified by sublimation at 65°C and then dried in a vacuum oven at room temperature. Deuterated biphenyl (Aldrich Chemical Company) was used as received. Toluene and DMAc were distilled from calcium hydride under nitrogen and stored over molecular sieves. Hexane and ethyl acetate (Aldrich Chemical Company) were used as received. *p*-Toluenesulfonhydrazide (Aldrich Chemical Company) was used as received. The NMR reagent $Cr(acac)_2$ was purchased from the Venton Company and used as received. The sodium chloride FT-IR grade salt plates were purchased from International Crystal Laboratories.

2.2. Synthesis of model compounds (I)–(III) (Schemes 1–3)

(I): A three-neck 250 ml round bottom flask equipped with a dean stark trap, reflux condenser, magnetic stir bar,

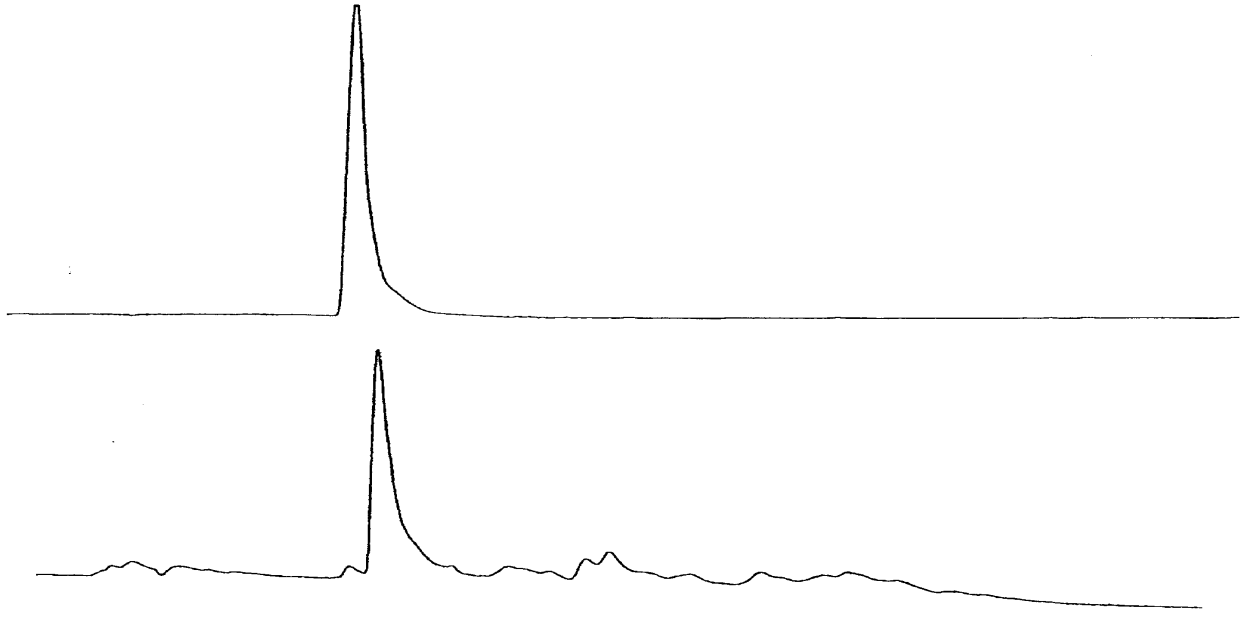

Fig. 2. HPLC traces of model compounds (I) and (II) cured for 30 min at 375°C.

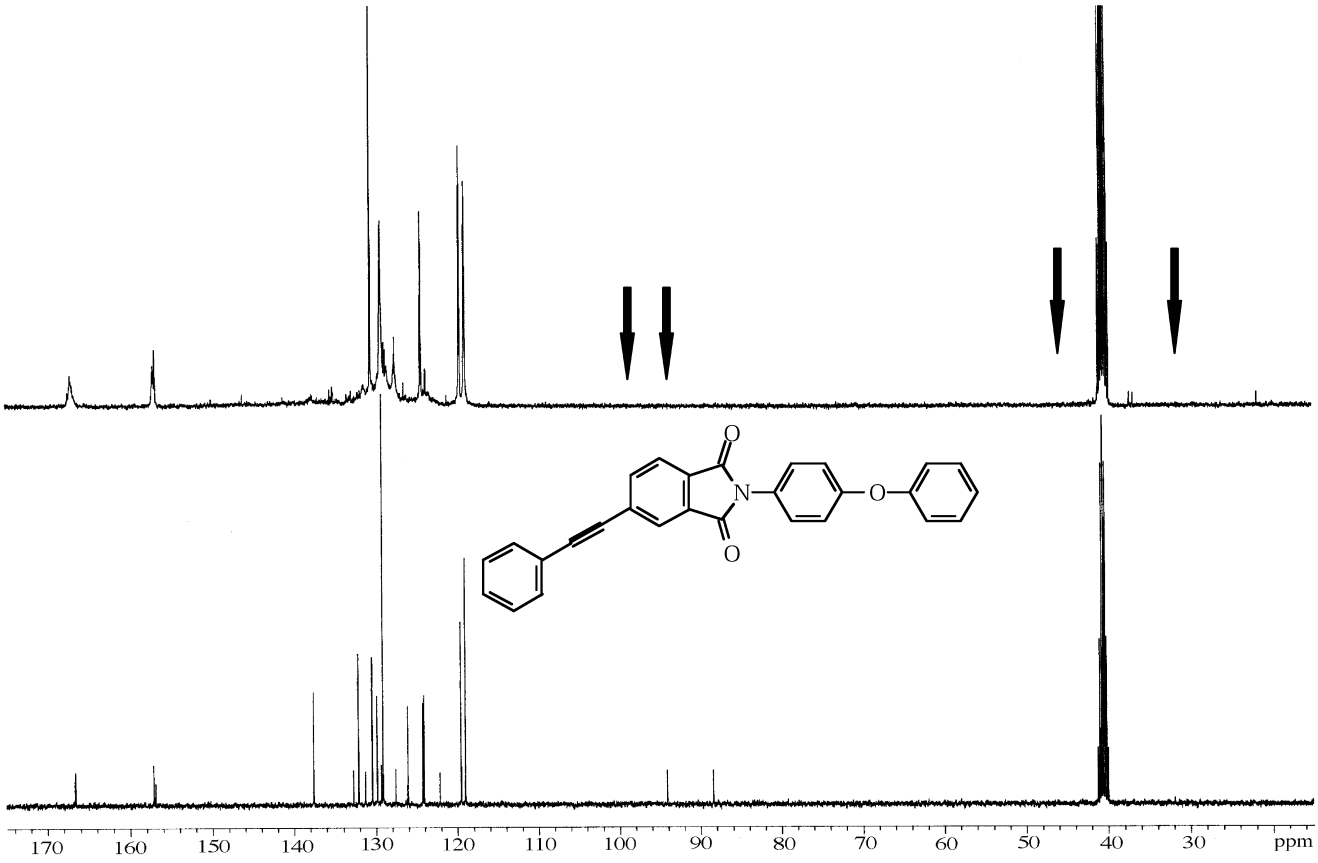

Fig. 4. ^{13}C NMR spectra of model compounds (I), (II) and (III) cured for 1 h at 375°C under nitrogen.

a nitrogen inlet and outlet was used. The 4-PEPA (8.400 g, 3.39×10^{-2} mol), 4-POA (6.272 *g*, 3.39×10^{-2} mol), toluene (50 ml) and DMAc (50 ml) were added to the flask. The solution was heated to 135°C for 6 h under nitrogen and the water formed was collected in the dean stark trap. As the solution cooled, the product precipitated from solution. It was collected by vacuum filtration, washed with ether and dried in a vacuum oven at 110°C for 24 h; yield = 90%, m.p. = 236–237°*C*. Elemental analysis: calculated for $C_{28}H_{17}NO_3$: C 80.95; H 4.12; N 3.37; O

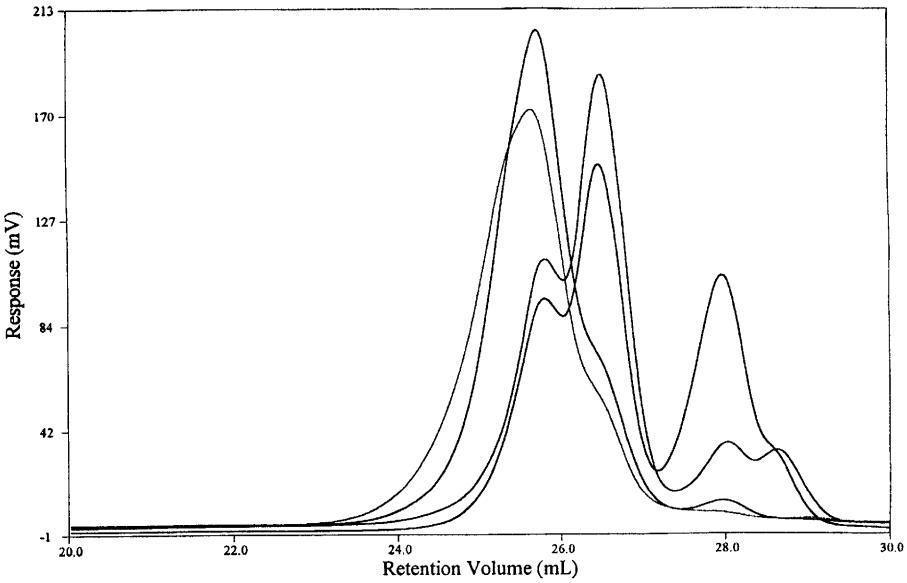

Fig. 5. GPC traces of a crude cured sample and fractions A–D.

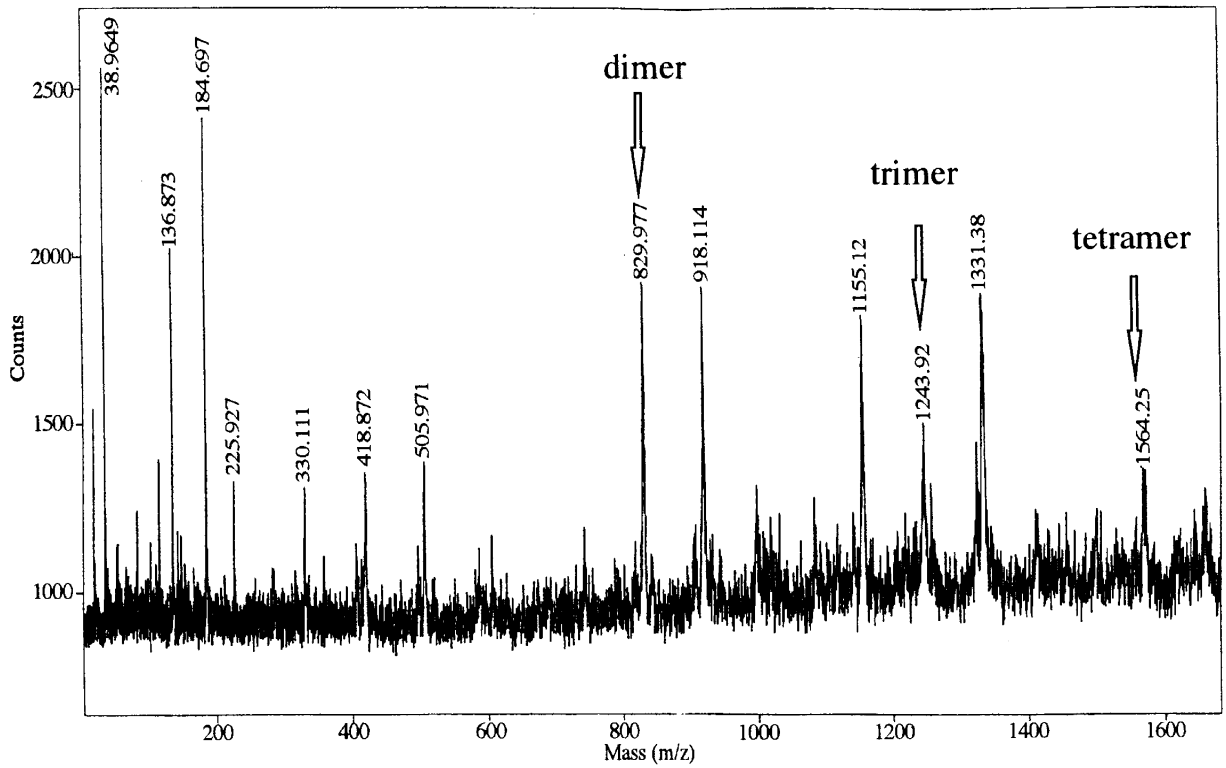

Fig. 6. MALDI-TOF MS of the first fraction (A).

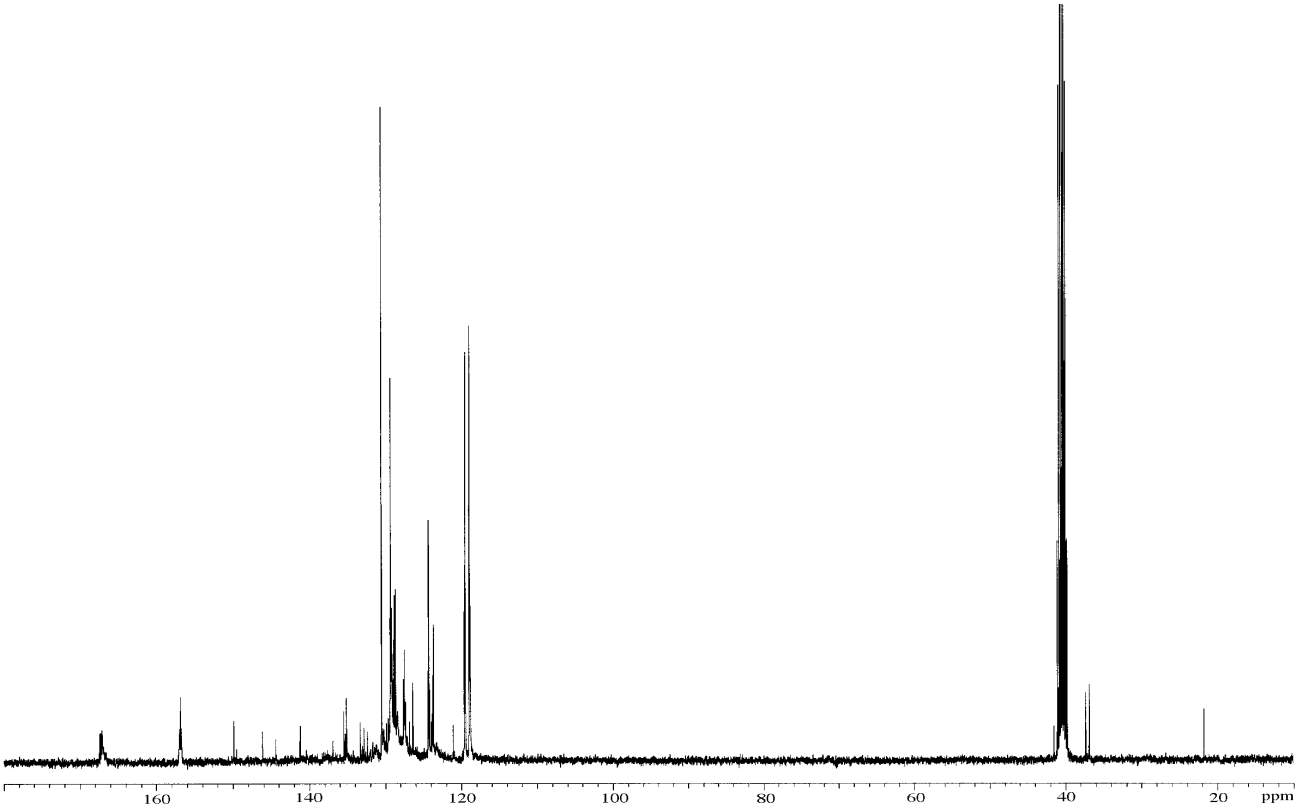

Fig. 7. ^{13}C NMR spectrum of model compound (I).

Table 2
Molecular weight data from GPC in chloroform for the 375°C h^{-1} reaction product and the four fractions

Sample	M_n (g mol^{-1})	M_w (g mol^{-1})	M_w/M_n
Crude	1200	1310	1.2
A	600	870	1.4
B	610	830	1.4
C	1240	1400	1.3
D	1460	1670	1.1

11.56; found: C 80.92; H 4.14; N 3.23; O by difference 11.71. IR (KBr) 3046 cm^{-1} (s, aromatic C–H), 2214 (m, phenylethynyl), 1778 (s, imide), 1587 (s, aromatic), 1393 (vs, aromatic, 1243 (s, aromatic ether), 714 (w, imide).

(II): A three-neck 100 ml round bottom flask equipped with a dean stark trap, reflux condenser, magnetic stir bar, a nitrogen inlet and outlet was used. The 4-MPA (0.5484 g, 3.38×10^{-3} mol), 4-POA (0.6283 g, 3.39×10^{-3} mol), toluene (10 ml) and DMAc (10 ml) were added to the flask. The rest of the procedure was the same as for (I); yield = 60% (not optimized). m.p. = 179–180°C. Elemental analysis: calculated for $C_{21}H_{15}NO_3$: C 76.60; H 4.60; N 4.30; O 14.50; found C 76.90; H 4.89; N 4.14; O by difference 14.07. IR (KBr) 3077 (w, aromatic C–H), 2919 (w, aliphatic C–H), 1779 (s, imide), 1609 (m, aromatic), 1393 (vs, aromatic), 1248 (vs, aromatic ether), 714 (w, imide).

(III): Compound (III) was prepared by reduction of the triple bond in (I) using *p*-toluenesulphonhydrazide, a source of diimide [26,27]. Model compound (I) (0.6040 g, 1.45×10^{-3} mol) was added to a 250 ml single neck round bottom flask equipped with a magnetic stir bar, reflux condenser, nitrogen inlet and outlet. *o*-Xylene (50 ml) was added to the round bottom flask and the apparatus was heated to 110°C until (I) dissolved. The solution was removed from the oil bath and the *p*-toluenesulfonhydrazide (1.6213 g, 8.72×10^{-3} mol) was added to the solution. The mixture was returned to the oil bath and the temperature was raised to 135°C and maintained for 8.5 h. The apparatus was removed from the oil bath and immediately hot filtered through fluted filter paper. As the filtrate cooled, more material precipitated and the mixture was again filtered. The combined precipitates were dried overnight at 100°C. The crude precipitates were purified by rinsing the precipitate in a fritted glass filter with ethanol followed by diethyl ether to remove impurities of *p*-toluenesulfinic acid. The purified

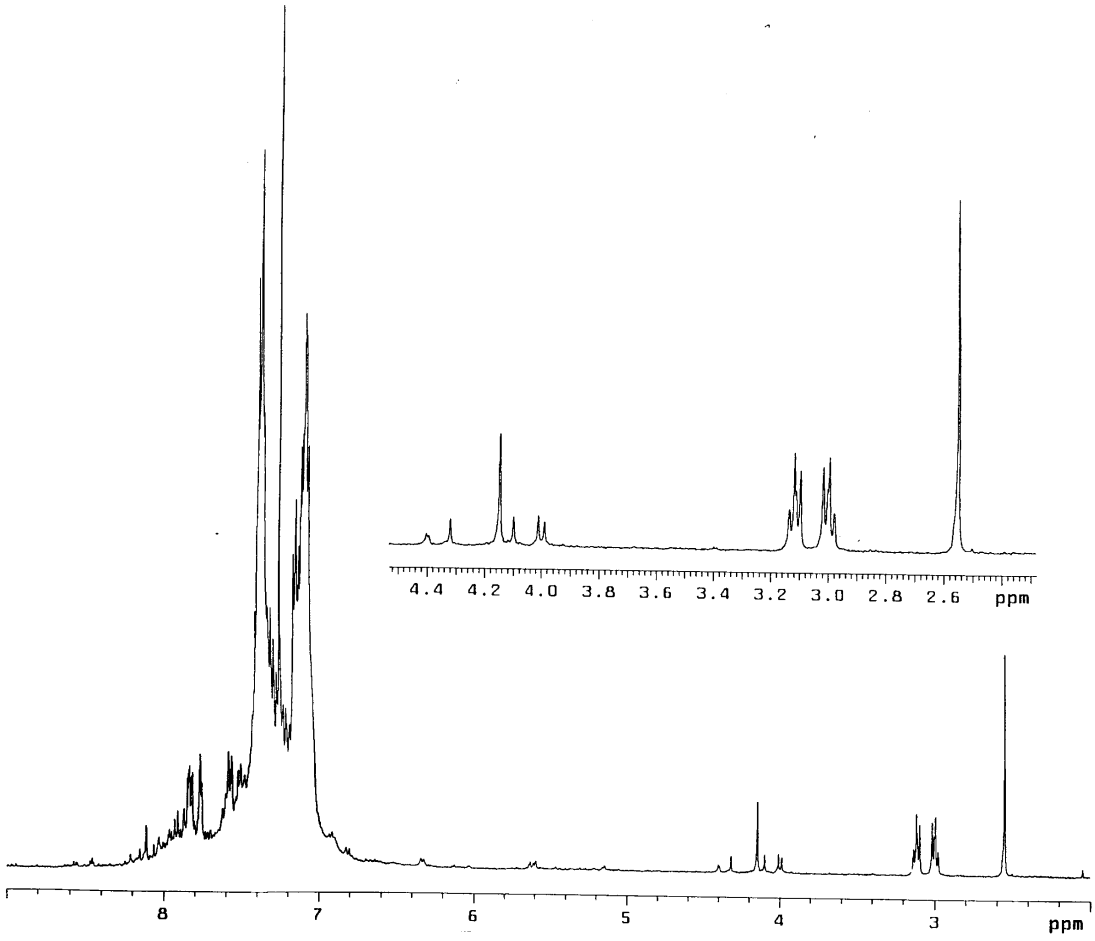

Fig. 8. ^{1}H NMR spectrum of the first fraction (A).

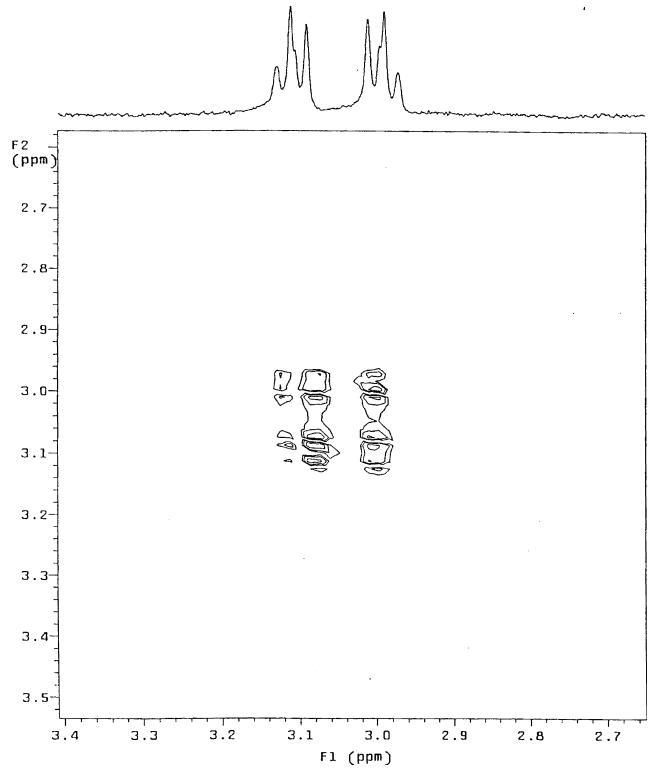

Fig. 9. DQCOSY of the first fraction (A).

product was then dried overnight at 100°C. m.p. = 228–229.5°C Elemental analysis: calculated for $C_{28}H_{21}NO_3$: C 80.17; H 5.04; N 3.34; O 11.45; found: C 80.38; H 5.27; N 3.25: O by difference 11.10. IR (KBr) 3057 cm^{-1} (w, aromatic C–H), 2927 (w, aliphatic C–H), 1776 (s, imide), 1587 (S, aromatic), 1489 (s, aromatic), 1243 (s, aromatic ether).

2.3. Curing procedure

About 0.3–0.4 g of (I) was added into a glass reaction vessel. The vessel was sealed with a rubber septum and fastened with copper wire. The vessel was purged with nitrogen or oxygen for 10–15 min, or in the case of an air atmosphere, not purged at all. For the samples which were cured under high vacuum, the glass reaction vessel was attached to a high vacuum line with a diffusion pump. The vacuum was reduced to at least 10^{-5} Torr, then purged with argon. This was repeated three times for 3–4 h in an attempt to remove all oxygen. The glass vessels were then sealed using a butane/oxygen torch. The resulting glass ampoule was put into a Thermolyne type 47900 furnace at 325–375°C under nitrogen flow. After the specified time, the ampoule was allowed to cool, then broken open to collect the contents.

2.4. Characterization

All NMR experiments were obtained from a Varian Unity 400 MHz spectrometer. The experiments were performed using 50 mg of material in 0.75 ml of DMSO-d_6 (or $CDCl_3$) at 20–120°C in a 5 mm NMR tube. The HMQC, APT and DQCOSY spectra were obtained using standard pulse sequences. The HMBC spectrum was performed using the standard HMBC pulse sequence using phase cycling [28]. The HMBC experiment was optimized for a 9 Hz H–^{13}C coupling. The thin-layered chromatography (TLC) and column chromatography experiments were performed using silica gel and a mixture of ethyl acetate (0–60%) in hexane. The high performance liquid chromatography (HPLC) experiments were performed using a Varian Vista 5500 LC using acetonitrile/H_2O as the mobile phase. Gel permeation chromatography (GPC) measurements were performed on a Waters GPC using a M590 pump with a differential refractometer detector (Viscotek Laser DRI) and an on-line differential viscometric detector (Viscoteck DV100). The columns used were Waters Styragel HR1 + HR2 + HR4 using a chloroform mobile phase at 30°C with a flow rate of 1 ml min^{-1}. The differential scanning calorimetry (DSC) measurements were performed using a Perkin–Elmer DSC-7 under nitrogen at a heating rate of 10°C min^{-1}. The MALDI-TOF mass spectrometry (MS) experiment was performed using a 2,5-dihydroxybenzoic acid matrix at Washington University Mass Spectrometry Resource. Elemental analysis was performed by Galbraith Laboratories. MS results were performed on a VG 7070 E-HF (micromass) high resolution, double focusing, magnetic sector mass spectrometer. The probe

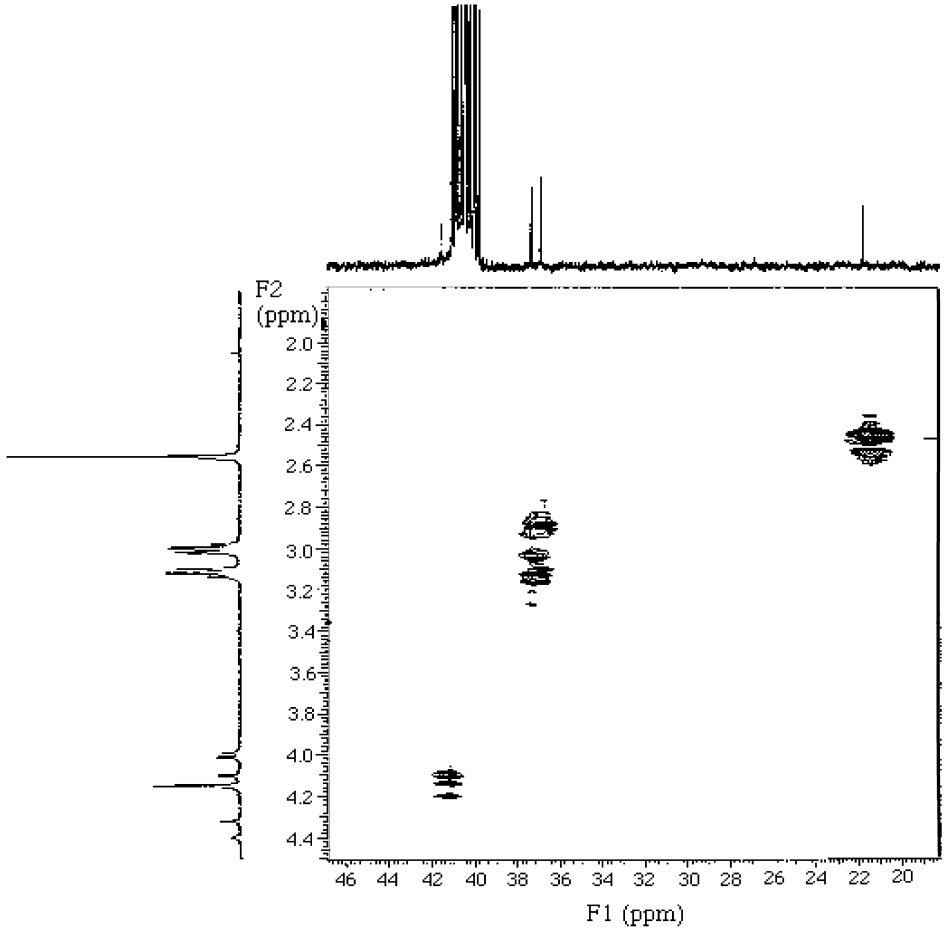

Fig. 10. HMQC spectrum of the first fraction (A).

temperature was ramped from 20 to 400 or 550°C at 5°C s^{-1}. A 70 eV electron impact ionization was used and a scan range of 750–50 amu and a scan rate of 5 s dec^{-1}. The rest of the reported mass spectral analysis were obtained from a VG Quattro (micromass) triple stage quadrupole mass spectrometer. The probe temperature was ramped from 30 to 400°C at 5°C s^{-1}. A 70 eV electron impact ionization was used and a scan range of 650–50 amu and a scan rate of 2 s $scan^{-1}$.

2.5. Kinetics

2.5.1. NMR

The quantitative ^{13}C NMR experiments were performed on samples of model compound (I) reacted in glass ampoules under the specified conditions of air, nitrogen, oxygen or high vacuum atmosphere. The quantitative ^{13}C NMR experiments were performed using about 300 mg of soluble cured material in a 3.0 ml solution of $Cr(acac)_2$ in DMSO-d_6 using a 10 mm NMR tube. A total delay time was set to 6 s and a standard gated decoupler was used. The conversion of the phenylethynyl group was determined by integration of the 2-phenylethynyl resonances at $\delta_C = 89$ and 94 ppm and compared to three different regions of aromatic carbon resonances. The three regions are from $\delta_C = 165$–168 ppm (two carbons), $\delta_C = 156$–158 ppm (two carbons) and from $\delta_C = 118$–120 ppm (four carbons). Reported conversions of the phenylethynyl group were determined by the average of these six values and the standard deviation was used for the error.

2.5.2. Fourier transformed infrared study

The rate of disappearance of the phenylethynyl stretch at 2214 cm^{-1} at specified temperatures was performed using a Nicolet Impact 400 FT-IR spectrometer. A sample of model compound (I) (70–80 mg) was placed in between two NaCl FT-IR grade salt plates and inserted into a heated sample holder, which was placed in the spectrometer. The sample was heated to the desired temperature and scans were collected using the Omnic Series software for 40–60 min from 315 to 335°C. All spectra collected were normalized using the aromatic carbon–hydrogen stretch at 3046 cm^{-1}. The area of the phenylethynyl vibration was measured and used as a determination of the concentration at any given time.

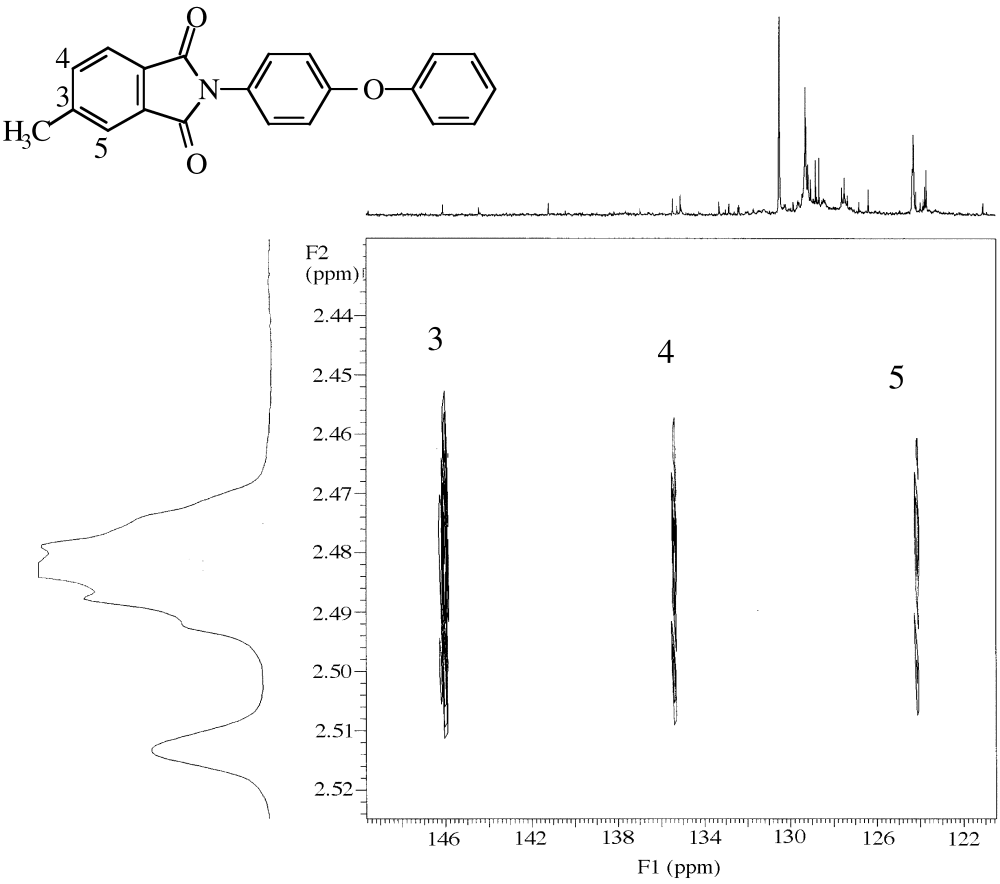

Fig. 11. HMBC spectrum of the first fraction (A).

3. Results and discussion

3.1. Synthesis of the model compound

The curing characteristics of the phenylethynyl terminated oligomers were investigated using model compounds in order to characterize more easily the reactions of these end groups under homogeneous conditions. An aryl ether imide model compound (I) (molar mass = 415.45 g mol^{-1}) was prepared by the reaction of 4-PEPA and 4-POA. This compound was designed to model a typical polyimide end group containing a 4-PEPA endcapper.

The ^{13}C NMR spectrum of the imide model compound is shown in Fig. 1. The spectrum clearly shows the phenylethynyl carbon resonances at $\delta_C = 89$ and 94 ppm and the aromatic carbon resonances appear from $\delta_C = 118$–160 ppm. All of the resonances are assigned to the carbon atoms number in (I) above and shown in Table 1. Compound (I) was the principal model used for the study of the thermal reaction of the phenylethynyl moiety described in this article.

The model compound was cured at a typical temperature (375°C) suitable for the curing of the oligomer. For example, a typical curing temperature for an oligomer might be 370°C for 60–90 min [3–7]. The model compound was thermally treated at 375°C for 30 min under nitrogen. HPLC was performed on this sample and model compound (I) (Fig. 2). A variety of different species are present in the sample including unreacted (I), and separation of these different species may be possible by chromatography. The model compound (I) was then further reacted at 375°C for 1 h. This sample was now an amorphous glass, but was soluble in a number of solvents including DMSO, in contrast to the usual oligomers which bear two or more phenylethynyl groups and produce a high gel fraction thermoset [4]. This result indicates that the single phenylethynyl reactive end group is behaving essentially in a difunctional manner.

The thermal behavior of model compound (I) and material cured at 325°C under nitrogen was investigated using DSC. Fig. 3 shows the DSC traces of (I) and samples cured for 30, 60 and 90 min at a scan rate of 10°C min^{-1}. Model compound (I) shows a sharp melting endotherm at 235°C, the cured samples show that the melting endotherm decreases in temperature and width as the cure time increases. The sample cured for 90 min indicates only a T_g that is over 200°C.

The ^{13}C NMR spectrum of (I) and the cured model compound (I) is shown in Fig. 4. Disappearance of the resonances at $\delta_C = 89$ and 94 ppm due to the phenylethynyl

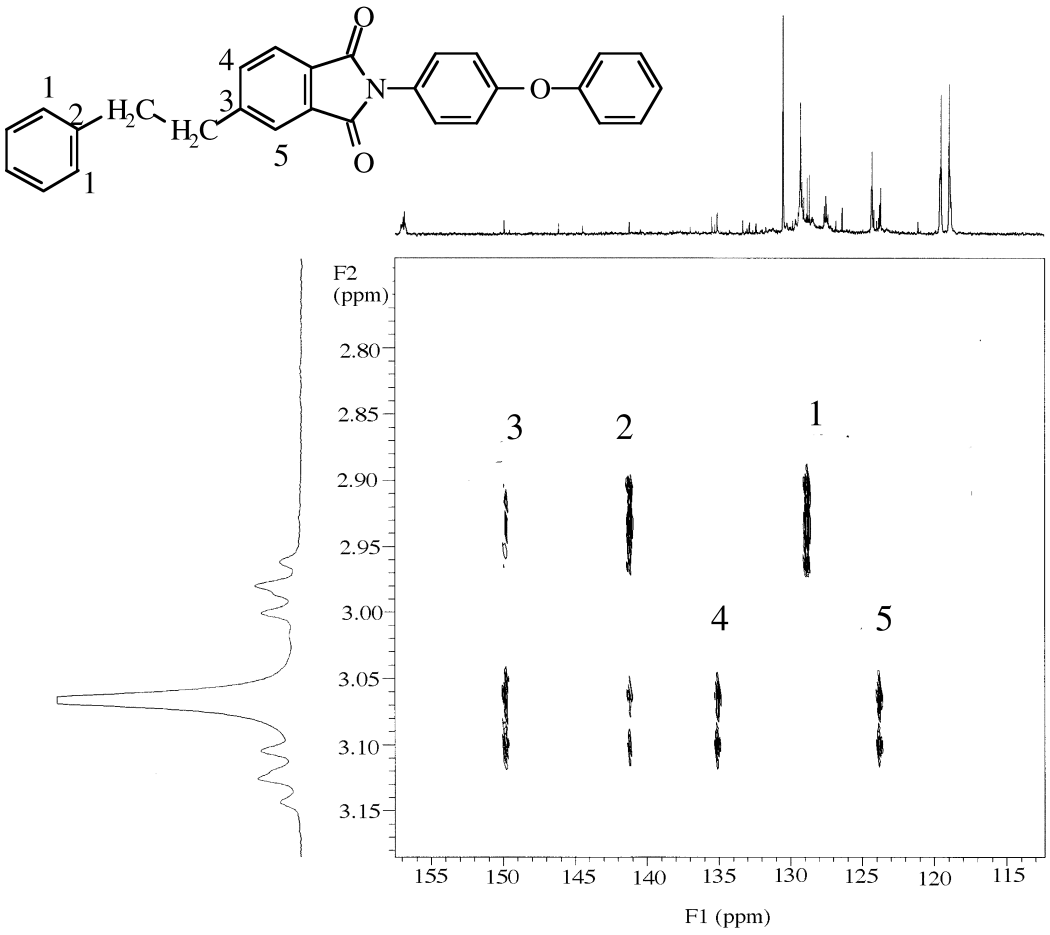

Fig. 12. HMBC spectrum of the first fraction (A).

group are noted, which indicates a high degree of reaction under these conditions. Many of the aromatic carbon resonances have began to broaden, indicating higher molecular weight species are present and many new resonances can be observed in this region. Another interesting result is that new peaks can be observed at $\delta_C = 21.8$, 36.6, 37.2 and 41.5 ppm, which surprisingly are in the aliphatic carbon region. This was an unexpected result due to the fact that no aliphatic carbon atoms are present in model compound (I) and, therefore, these products must reflect some aspects of the high temperature reactions.

As this sample is soluble at complete conversions and the HPLC trace (Fig. 2) shows a mixture of products, isolation was possible using column chromatography. The crude thermally cured sample was separated using a column of silica gel and hexane/ethyl acetate as a mobile phase. The polarity of the column was slowly raised by increasing the amount of ethyl acetate from 0 to 50%. All of the samples were combined into four different fractions (A–D) based on a similar R_f from TLC. Table 2 shows the molecular weight data obtained from the GPC traces (Fig. 5). These data in Fig. 5 indicate that the four fractions were generally separated by molecular weight. Further investigation focused mainly on the first fraction (A), which corresponds to about 13% of the overall material.

MALDI-TOF MS of the first fraction was performed in order to identify the structures and molar masses present in this fraction and the results are shown in Fig. 6. MALDI-TOF is designed to minimize fragmentation of higher molecular weight species which may complicate traditional MS experiments. Fig. 6 shows that there are a large number of different species present, including a number of different higher molecular weight materials. The model compound has a formula weight of 415 g mol^{-1}, which cannot be observed in this figure. Peaks for the dimer (830 *m*/*z*), trimer (1244 *m*/*z*) and tetramer (1662 *m*/*z*) are clearly present. In addition to these expected structures, higher molecular weight species that do not correspond to an integral multiple of the formula weight of model compound (I) are also present. These structures are from 87–91 *m*/*z* different than the integral mass peaks. In addition to these higher molecular weight species, lower molecular weight peaks are also present. These peaks appear at 330, 419 and 506 *m*/*z*. It was considered that these peaks may be due to a structure which are fragments of the model compound (I). They are also not due to the matrix or

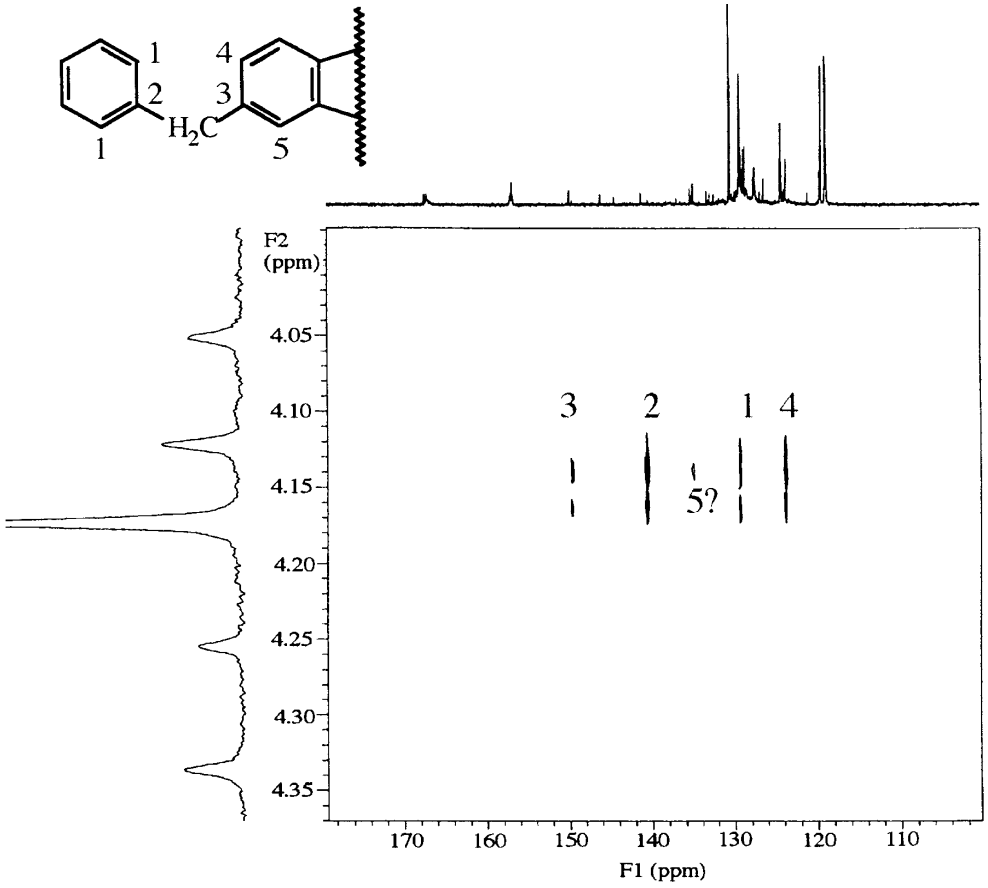

Fig. 13. HMBC spectrum of the first fraction (A).

an artifact of the instrument, like the peaks at 226 *m/z* and lower.

The ^{13}C NMR spectrum of the first fraction is shown in Fig. 7. This spectrum is much different from that of the crude cured sample shown in Fig. 4. For example, Fig. 7 shows additional resonances between $\delta_C = 135$–155 ppm which are not present in the spectrum of the model compound (Fig. 1) and barely visible in the spectrum of the crude thermally cured sample (Fig. 4). The resonances in the aliphatic carbon region are much more intense than those in Fig. 4. They are very sharp, which would seem to indicate a more mobile or lower molecular weight species. This conclusion is supported by the GPC results indicated in Table 2. A DEPT spectrum was performed on the first fraction which indicates that the resonance at $\delta_C = 21.8$ ppm is due to a carbon atom with three attached protons and the resonances at $\delta_C = 36.6$, 38.2 and 41.5 ppm are due to carbons with two attached protons.

The corresponding ^1H NMR spectrum of the first fraction is shown in Fig. 8. In the region of aromatic proton resonances from $\delta = 6.7$–8.5 ppm, little information can be extracted due to the complexity of this region, but a number of new resonances are present from $\delta =$ 2.4–4.5 ppm. They are in the region where aliphatic protons are normally observed. Singlet proton resonances are observed at $\delta = 2.56$ ppm and also in the region of $\delta =$ 3.9–4.5 ppm. This indicates the presence of isolated protons without adjacent nonequivalent protons and a pair of triplets are evident from $\delta = 2.9$–3.2 ppm. The unsymmetrical shape of these triplets indicates that they are two adjacent nonequivalent methylene protons. A DQCOSY spectrum of the first fraction (Fig. 9) was performed in order to show that the triplets are adjacent to one another. The presence of the four crosspeaks indicates that these two sets of protons are on adjacent carbon atoms.

The next step in identifying the structures present in this first fraction was to attempt to formulate connectivities of protons and carbons. The HMQC spectrum shows crosspeaks for protons and carbons attached through one bond (Fig. 10). The carbon resonance at $\delta_C = 21.8$ ppm, which was shown in the DEPT spectrum to correspond to a carbon atom containing three attached protons, shows a correlation to the singlet proton resonance at $\delta = 2.56$ ppm. These resonances are in the region that corresponds to a methyl group attached to an aromatic ring. The carbon resonances at $\delta_C =$ 36.6 and 37.2 ppm, which were shown in the DEPT spectrum to correspond to a carbon atom containing two attached protons and display a correlation to the two triplet proton resonances from $\delta = 2.9$–3.2 ppm. This evidence would indicate the presence of two adjacent nonequivalent

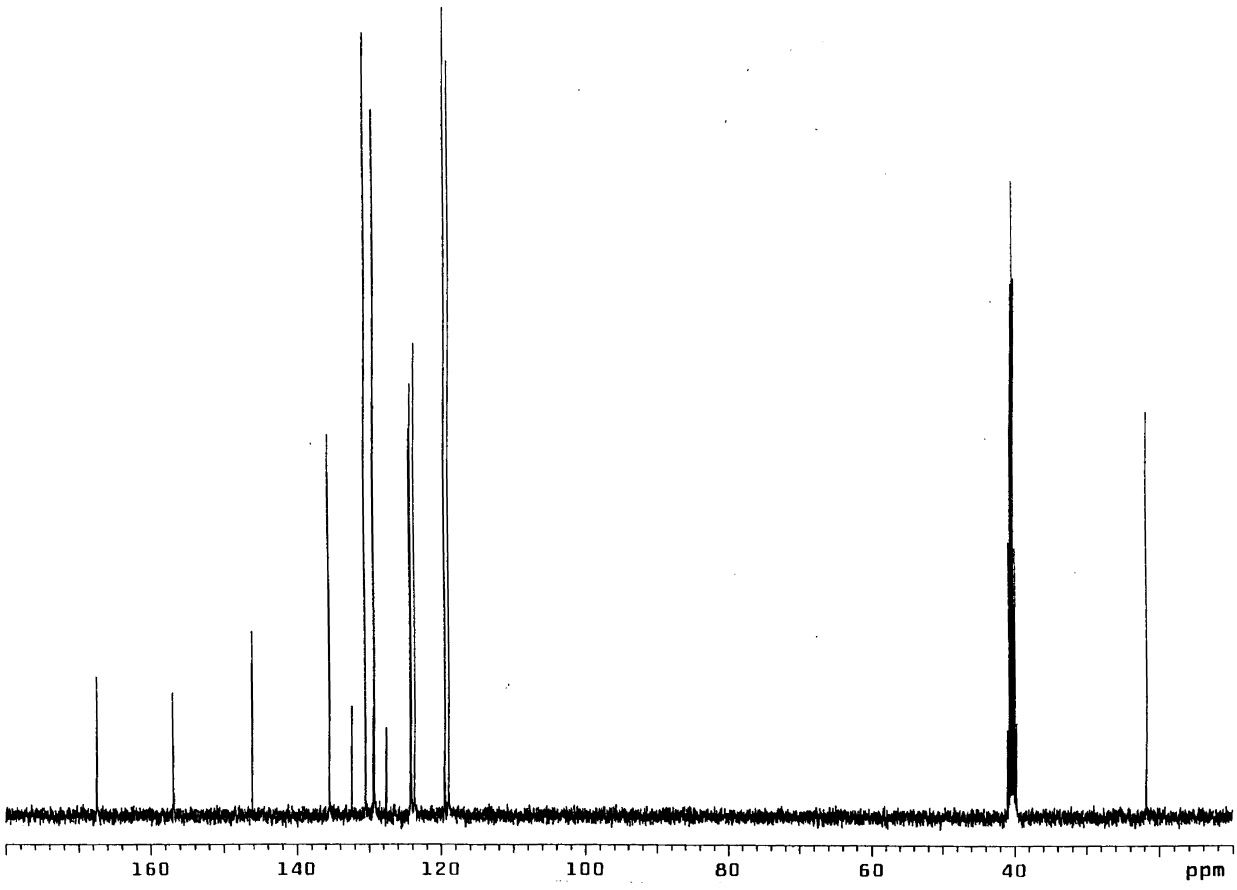

Fig. 14. ^{13}C NMR spectrum of fragment (II).

methylene units. The carbon resonance at $\delta_C = 42$ ppm, which was shown in the DEPT spectrum to correspond to a carbon atom containing two attached protons, has a correlation to one of the proton resonances in the region of $\delta =$ 3.9–4.4 ppm. This evidence would indicate the presence of a methylene carbon between two aromatic rings. The ^{13}C, ^{1}H, DEPT and HMQC NMR spectra suggest the presence of three fragments shown below.

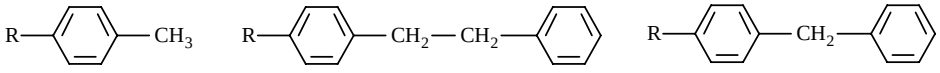

The next step in identifying the origin of these aliphatic resonances is to look at long range correlations to these aliphatic proton resonances. The HMBC pulse sequence is able to correlate carbons attached to protons through two or three bonds. The HMBC spectrum of the first fraction in the range of the aliphatic methyl proton resonance at $\delta =$ 2.51 ppm is shown in Fig. 11. It shows crosspeaks at $\delta_C =$ 146, 135 and 124 ppm which correspond to carbon atoms which are two or three bonds away from the methyl protons. The structure of the proposed fragment of the model compound is also given in Fig. 11. These three crosspeaks correspond to a two-bond correlation to the carbon atom labeled 3 ($\delta_C = 146$ ppm) and two three-bond correlations that correspond to the carbon atoms labeled 4 ($\delta_C = 135$) and to the carbon atom labeled 5 ($\delta_C = 124$). The resonances for carbons 4 and 5 in Fig. 11 closely correspond to the same resonances of (I). This is a good evidence of the presence of fragment (II) in the cured sample. Also, if this fragment is a product of the curing reaction, then a peak in the MALDI-TOF MS should be present at the mass of this fragment ($m/z = 330$ Da). The MALDI-TOF MS shown in Fig. 6 does show a peak at this mass.

Fig. 12 shows the same HMBC spectrum, but in the region of the two adjacent methylene protons from $\delta =$ 2.95–3.15 ppm. The upfield triplet at $\delta = 2.95$ ppm shows three crosspeaks at $\delta_C = 150$, 141 and 129 ppm and corresponds to the carbon atoms labeled 3, 2 and 1, respectively. The downfield triplet at $\delta = 3.10$ ppm shows four crosspeaks at $\delta_C = 150$, 141, 135 and 124 ppm and corresponds to the carbon atoms labeled 3, 2, 4 and 5, respectively. The

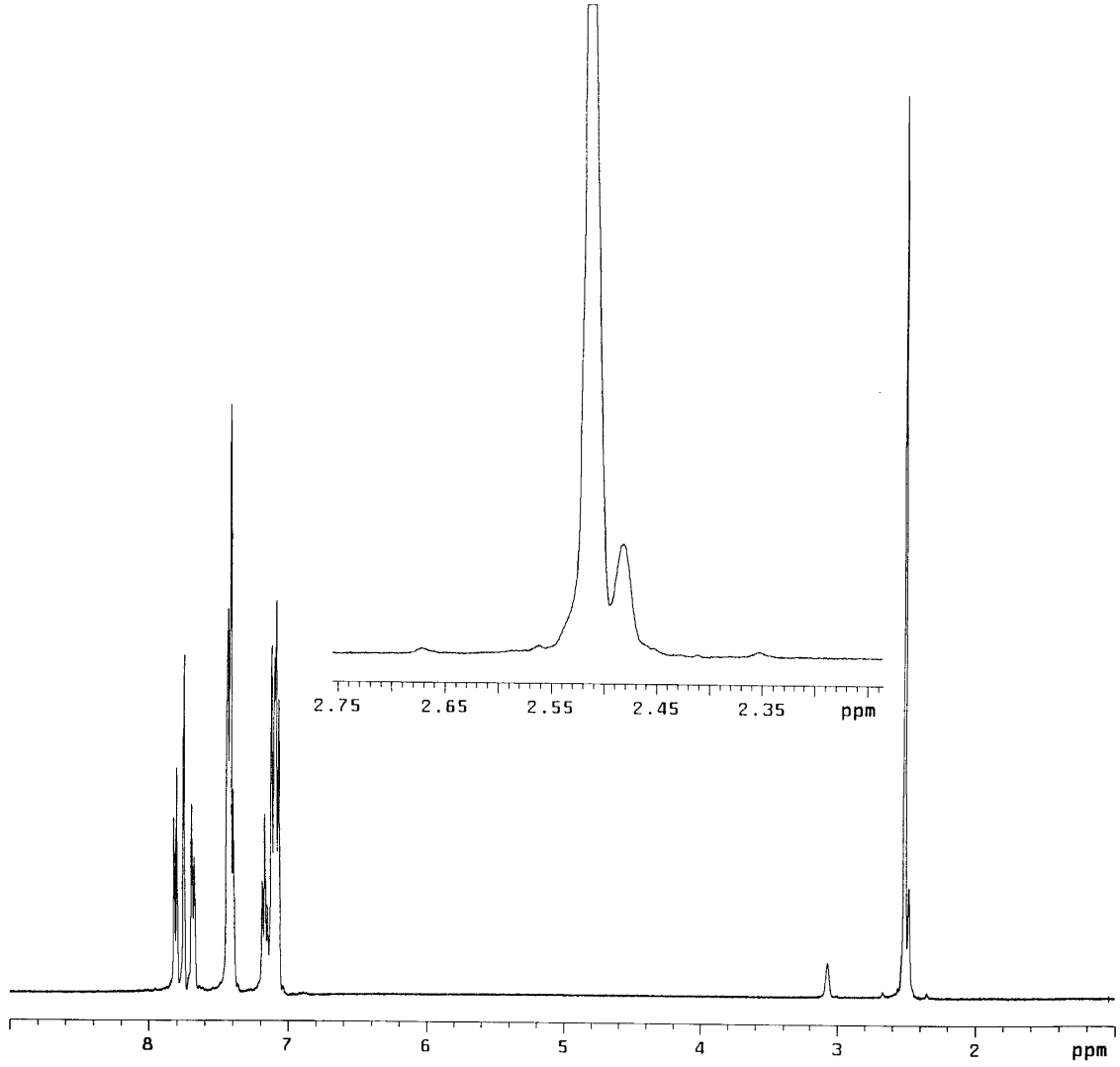

Fig. 15. ^{1}H NMR spectrum of fragment (II).

resonances for carbons 1, 4 and 5 in Fig. 12 closely correspond to the same resonances of (I) and (II). The structure of the proposed fragment (III) that contains these adjacent methylene units derived from the phenylethynyl group, is shown in Fig. 12. If this structure is present as a discrete compound derived from the model compound and not just for instance an end group, a peak in the MALDI-TOF MS (Fig. 6) should be present at 418 *m*/*z*. Thus, this structure is also present in the crude reaction product oligomeric mixture.

A third region of the HMBC spectrum from $\delta =$ 4.0–4.5 ppm is shown in Fig. 13. There are many proton resonances present in this region and no two resonances seem to be related through couplings. The largest singlet in this region at $\delta = 4.15$ ppm was determined to be due to an isolated methylene group, which suggests a probable structure shown in Fig. 13. This proton resonance appears to correlate to at least four different carbon resonances and perhaps five. If the above structure is correct, two-bond correlations should be present to carbon atoms labeled 2 ($\delta_C = 141$ ppm) and 3 ($\delta_C = 150$ ppm) and three-bond correlations should be present to carbon atoms labeled 1 ($\delta_C = 129$ ppm), 4 ($\delta_C = 124$ ppm) and 5 ($\delta_C =$ 135 ppm). These carbon chemical shifts also match with fragment (III). The correlation to carbon atom 5 is very weak and may not be a true crosspeak. There are also many other smaller peaks in the ^{1}H NMR spectrum in this region which also are probably due to the same sort of isolated methylene group. If this fragment of the model compound were present after curing, a peak at 404 *m*/*z* in the MALDI-TOF MS (Fig. 6) should be present, but in this case no such peak was observed. However, if these benzyl fragments were a part of the higher molecular weight material instead of as a fragment, a peak at 404 *m*/*z* may not be present. Instead, these benzyl fragments may account for the peaks that are 87–90 *m*/*z* away from the monomer, dimer, trimer, etc. Some evidence against this conclusion would be

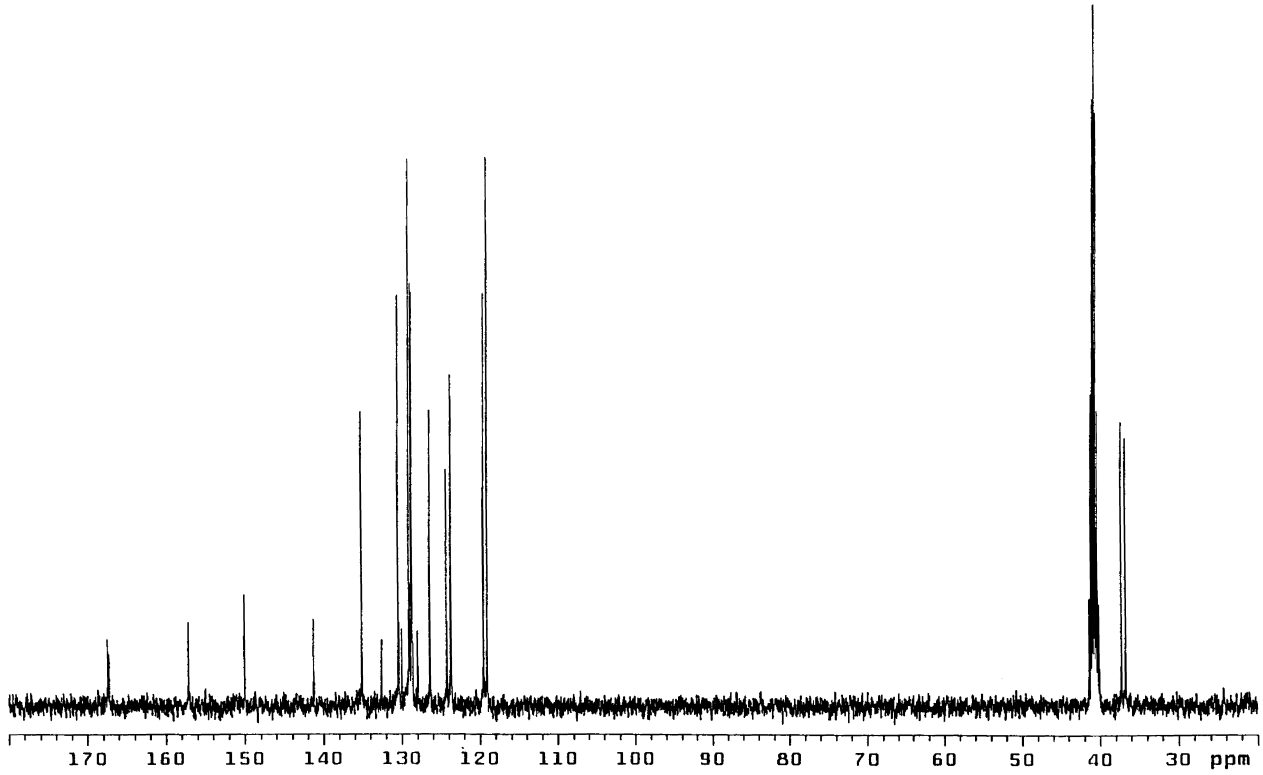

Fig. 16. ^{13}C NMR spectrum of model compound (II).

that the intensities of the ^{1}H NMR peaks are not nearly large enough to account for the apparent population shown in the MALDI-TOF MS.

Model compounds of some of the detected fragments were prepared by an alternative technique in order to determine if these are in fact the correct structures present in the cured model compound. For the first model compound, 4-methylphthalic anhydride was reacted with 4-POA to produce fragment (II) and the ^{13}C NMR spectrum is shown in Fig. 14. The spectrum shows the characteristic resonance due to the methyl carbon at $\delta_C = 21.8$ ppm, which is also present in the spectrum of the crude cured material (Fig. 4) and the first fraction (Fig. 7). Additional resonances which are characteristic to this fragment are present at $\delta_C = 124$, 135 and 146 ppm. These resonances can also be observed in the spectrum of the crude cured material (Fig. 4) and also as crosspeaks in the HMBC spectrum (Fig. 11). The ^{1}H NMR spectrum of this compound is shown in Fig. 15 and clearly shows the resonance due to the methyl protons at $\delta = 2.48$ ppm, which is also present in the ^{1}H NMR spectrum of the first fraction shown in Fig. 8. The methyl proton resonances in Figs. 8 and 15 do not exactly match because of different solvents and temperatures during acquisition. The EI mass spectrum of (II) indicates a peak at 330 *m/z*. The preceding experiments are excellent evidence that this fragment (II) is indeed formed during this curing reaction at these elevated temperatures.

The next fragment (III), can be formed easily by reduction of (I) by using such reagents as *p*-toluenesulphonhydrazide as a source of diimide to reduce the triple bond and not any aromatic rings or polar double bonds. The ^{13}C NMR spectrum of this reduced model compound (III) is shown in Fig. 16. It shows two carbon resonances at $\delta_C =$ 36.6 and 37.2 ppm due to the two nonequivalent methylene carbons. Additional resonances which are characteristic of the reduced model compound (III) are found at $\delta_C = 149$, 140, 134, 129 and 124 ppm. All of these carbon resonances are also found at the same chemical shift in the ^{13}C NMR spectrum (Fig. 7) and in the HMBC spectrum (Fig. 12) of the first fraction. The ^{1}H NMR spectrum of (III) is shown in Fig. 17. The resonances due to the two adjacent methylene carbons appear from $\delta = 2.8$–3.4 ppm. Again, these resonances are slightly different from the same resonances shown in Fig. 8 because of different NMR solvents and temperatures during acquisition. The EI mass spectrum of (III) indicates a peak at 419 *m/z*. The preceding experiments are excellent evidence that fragment (III) is indeed formed during this curing reaction at these elevated temperatures.

EI mass spectrometry was also performed on this sample cured at 375°C for 1 h. These experiments were performed by ramping the temperature of the probe while the cured model compound was on the probe. This program essentially separated the fragments by molecular weight or boiling point. A spectrum recorded at 2.86 min is shown in Fig. 18 and indicates the presence of peaks at 329 and 419 *m/z*, which is consistent with the mass of structures (II) and (III).

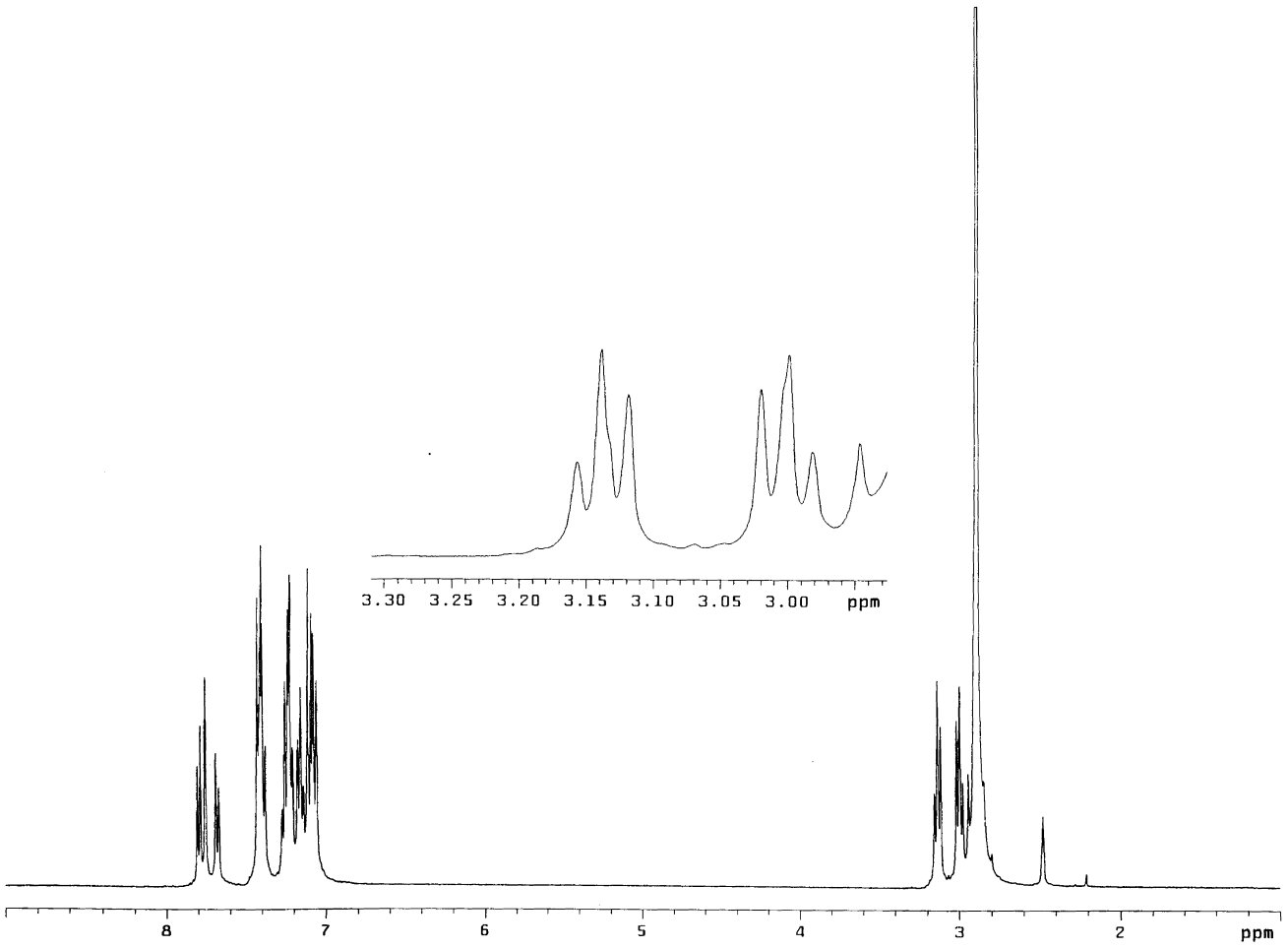

Fig. 17. ^{1}H NMR spectrum of fragment (III).

Also, a peak at 405 *m*/*z* is present indicating the presence of fragment (IV). Unfortunately, this peak could not be observed in the MALDI-TOF spectrum (Fig. 6). The peak at 315 *m*/*z* could indicate the presence of fragment (V). These two fragments, (IV) and (V) (Schemes 4 and 5), could also be due to fragmentation occurring in the spectrometer. Nevertheless, it appears that a variety of low molecular weight products are being formed during these high-temperature curing reactions.

A curious fact about these fragments is the presence of aliphatic protons. It is difficult to imagine an origin because of the lack of labile protons or even aliphatic protons in the model compound. One possible explanation might be that the reactive intermediates formed at these higher temperatures are able to abstract aromatic protons from the model compound. A possible method to test this theory was to co-cure (I) in the presence of an additive which contains aromatic deuterium atoms. This way, if deuterium were present in the cured model compound, it would have to come from the deuterated additive. This experiment could be complicated by the secondary isotope effect which dictates that if the abstraction of the deuterium atom could require more energy than abstraction of the hydrogen atom due to the difference in zero point energies [31]. Therefore, aromatic protons would be abstracted even in the presence of similar aromatic deuterium atoms.

Deuterated biphenyl (biphenyl-d_{10}) was co-cured in a 50/50 molar mixture with compound (I) at 375°C for 3 h under nitrogen. EI mass spectra were obtained from the cured mixture and indicated peaks at 164, 329 and 419 *m*/*z* as shown in Fig. 19. The peak at 164 *m*/*z* is due to the biphenyl-d_{10} and the peaks at 329 and 419 are due to fragments (II) and (III), respectively. The unreacted biphenyl-d_{10} was then separated by column chromatography using silica gel and hexane/ethyl acetate. The resulting crude cured model compound was then analyzed by a variety of different techniques. The EI mass spectra results indicate that the biphenyl-d_{10} is no longer present by the lack of a peak present at 164 *m*/*z*, while maintaining the peaks at 329 and 419 *m*/*z* as shown in Fig. 20. The ^{1}H NMR spectrum of the cured model compound after separation of the biphenyl-d_{10} is shown in Fig. 21 and shows a similar spectrum to the sample cured without biphenyl-d_{10} (Fig. 8). Both spectra show a very similar pattern of aliphatic resonances from $\delta =$ 2.4–4.5 ppm. The ^{2}H NMR spectra (Fig. 22) were obtained for both biphenyl-d_{10} and the cured model compound after

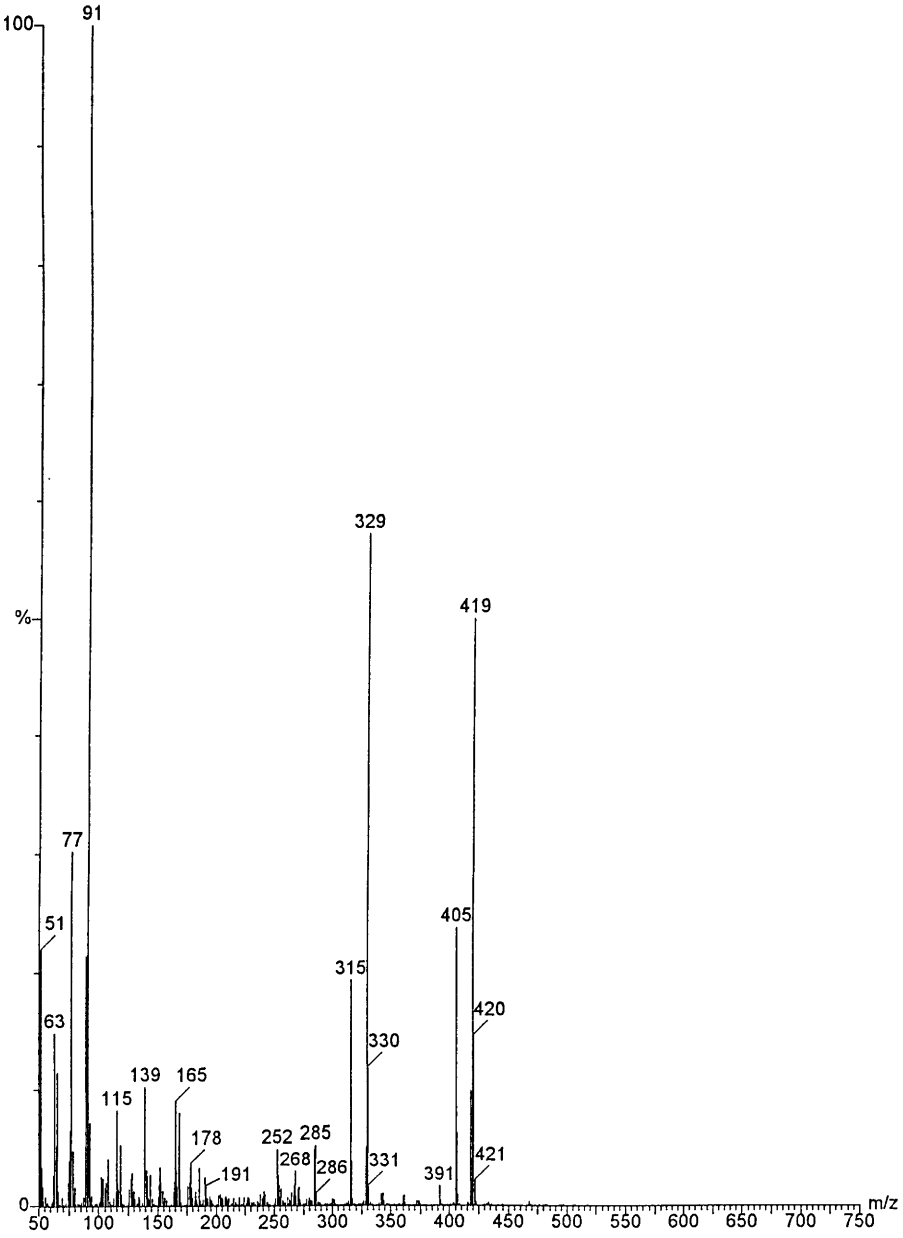

Fig. 18. EI mass spectrum of (I) cured for 1 h at 375°C.

separation of the deuterated biphenyl. The top spectrum, for biphenyl-d_{10}, shows only aromatic deuterium resonances and a small peak due to deuterated methylene chloride, an impurity in the NMR solvent. The bottom spectrum of the separated cured model compound indicates that most of the aromatic resonances are no longer present in the model compound spectrum, but some unknown resonances are still present, even though the MS results would indicate that these are not due to biphenyl-d_{10}, but perhaps some of the deuterium atoms were transferred to the aromatic rings of the model compound. The resonance due to the methylene

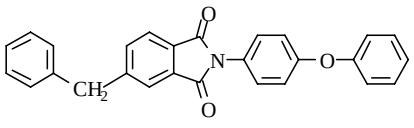

IV

Scheme 4.

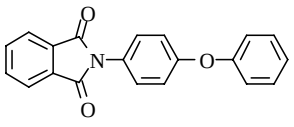

V

Scheme 5.

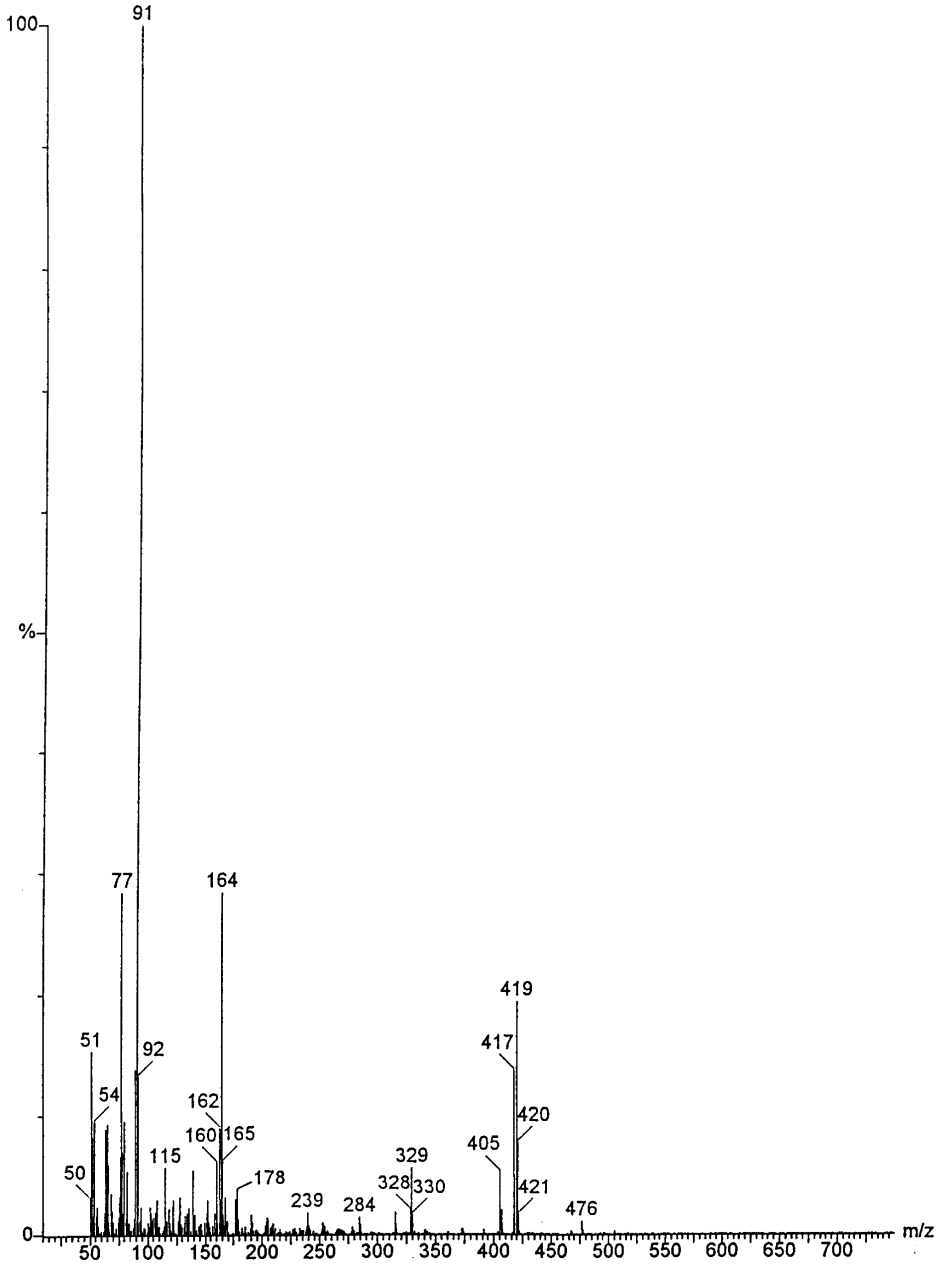

Fig. 19. EI mass spectrum of (I) co-cured with biphenyl-d_{10} at 375°C for 3 h.

chloride solvent is still present at $\delta_D = 5.5$ ppm, and a clear deuterium resonance can be observed at $\delta_D = 2.5$ ppm. This is at the same position as the methyl proton resonance of fragment (II) as indicated in Figs. 8 and 15. This would seem to indicate that some of (II) formed during this curing reaction contains some deuterium atoms attached to the methyl carbon of this fragment. The only possible origin of these deuterium atoms has to be the biphenyl-d_{10}. Some other resonances may be present at $\delta_D = 2.8$–3.0 ppm. These resonances would correspond to the methylene protons of fragment (III). EI mass spectra analysis was also performed on the product of this co-cure of the biphenyl-d_{10} and the model compound (I). Since the ^1H and ^2H NMR spectra indicate that fragment (II) contains both hydrogen and deuterium atoms at the methyl carbon, the relative intensity of the isotope peaks should support the presence of deuterium atoms and the relative amount. The results of the mass spectra analysis (Table 3) show the abundance of isotope peaks relative to the molecular ion for four different samples. The peaks due to fragment (II) (329 *m*/*z*) and (III) (419 *m*/*z*) were both investigated.

Theoretical calculations are based on the empirical formula for each fragment. The relative abundances of fragments (II) and (III) were determined from pure compounds. All the materials were cured at 375°C under nitrogen. The sample co-cured with biphenyl-d_{10} contained a much larger

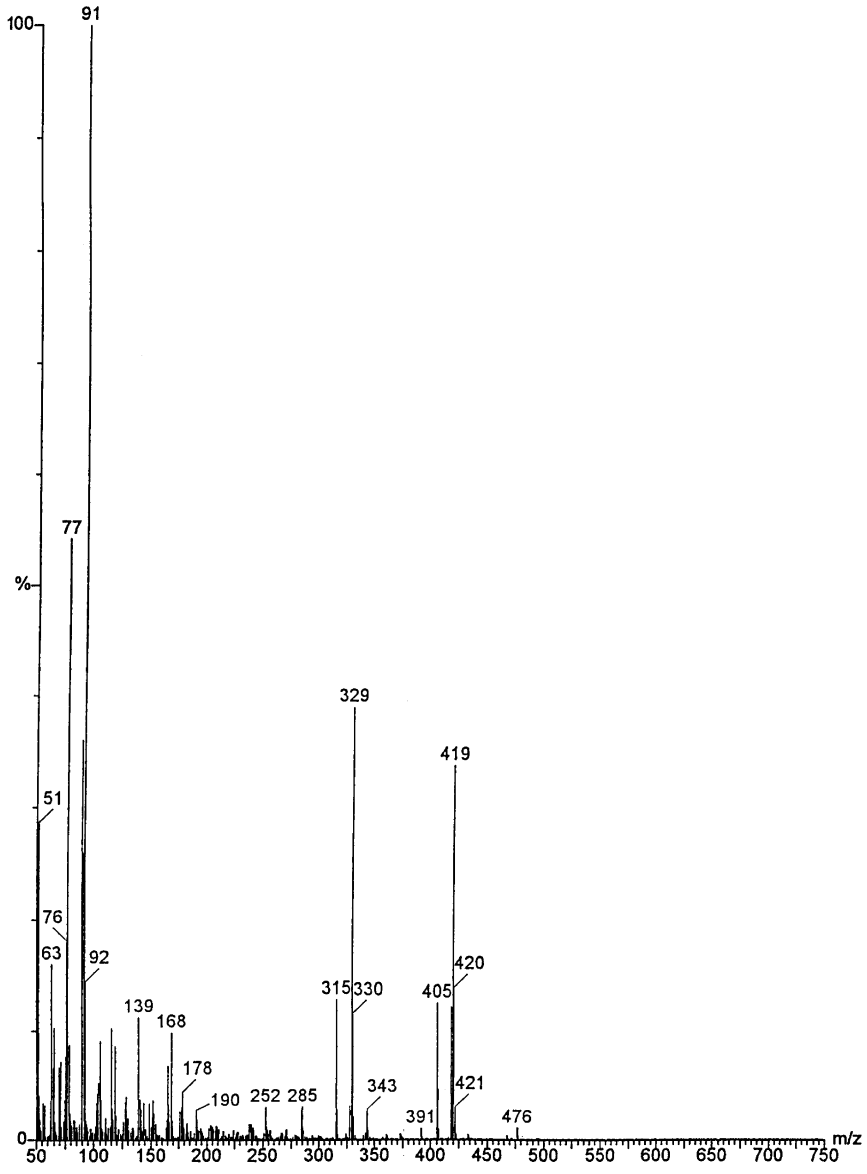

Fig. 20. EI mass spectrum of (I) co-cured with biphenyl-d_{10} at 375°C for 3 h; after extraction.

amount of the M + 1 isotope than any of the other samples. The mass spectra analysis of fragment (II), (III) and cured (I) contained a similar M + 1 and M + 2 isotope abundance to the theoretical values. This is a good evidence of the presence of deuterium atoms present in the cured sample of (I) in the presence of biphenyl-d_{10}.

These temperatures were recognized to be very high for the model compound and sublimation does occur at these temperatures. More mild reaction conditions of 325 and 350°C for longer times were attempted. The GPC and NMR experiments indicated a similar molecular weight and product distribution, with one exception. The resonances due to some of the aliphatic carbons are not present in the ^{13}C NMR spectra of samples cured at lower temperatures. Fig. 23 shows the ^{13}C NMR spectra of three samples cured at 375°C for 1 h, the middle spectrum at 350°C for 4 h and the bottom spectrum at 325°C for 9 h. These times are longer than necessary for complete cure. It is apparent that the resonances at $\delta_C = 22$ and 42 ppm are decreasing with decreasing cure temperature, although the resonances at $\delta_C = 36.6$ and 37.2 ppm are unchanged. These resonances are due to fragment (III).

Once these fragments had been determined by a variety of techniques, the next question was that what is the function of these fragments? Are they solely a side product or are they involved in the initiation or propagation reactions. The pure compounds of fragments (II) and (III) were cured separately at 325°C under nitrogen for 5 h. These conditions would produce, when applied to model compound (I), a fully reacted compound (i.e. devoid of resonances at $\delta_C =$ 89 and 94 ppm). When fragments (II) and (III) were subjected to these conditions, no reactions occurred as

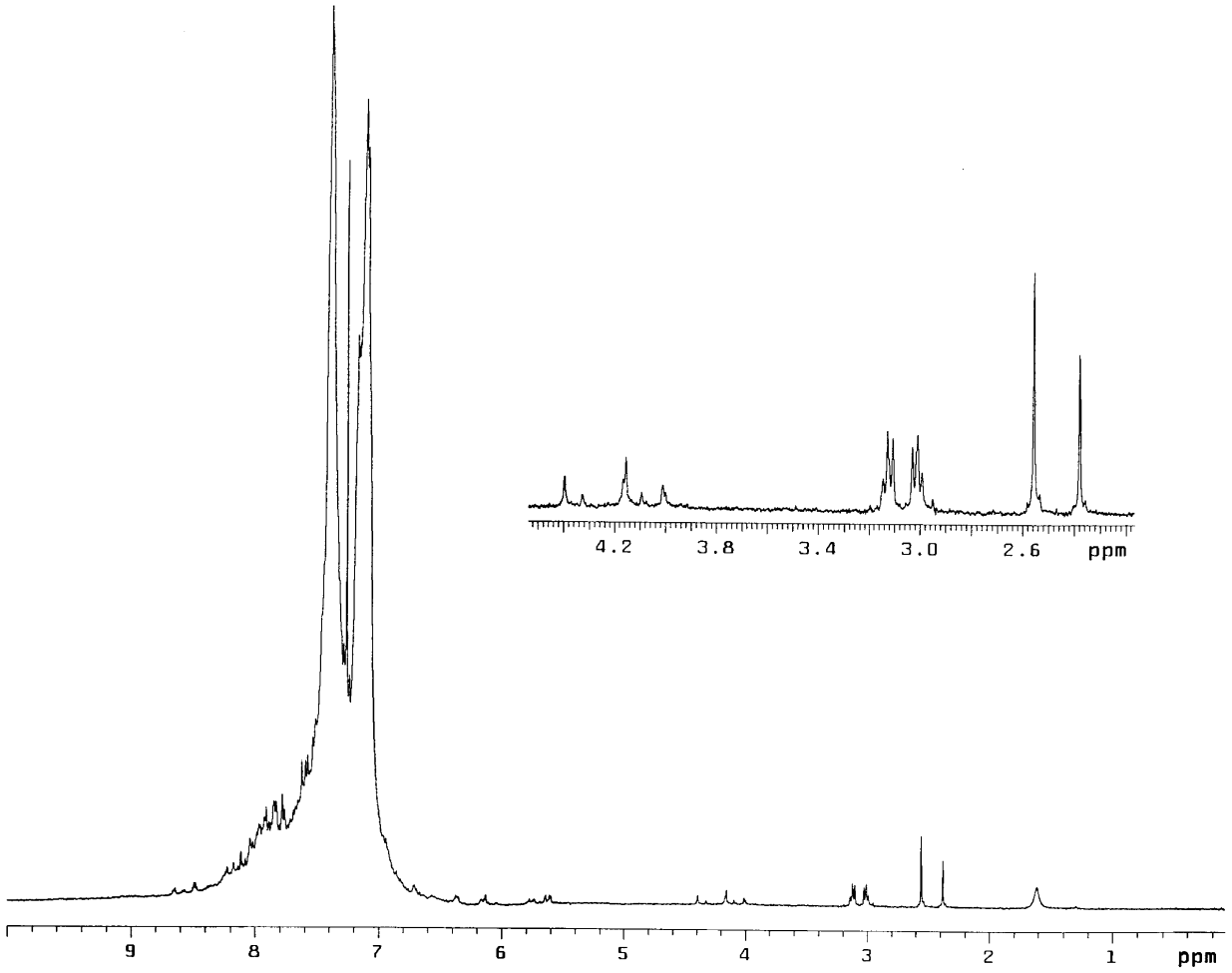

Fig. 21. ^{1}H NMR spectrum of (I) co-cured with biphenyl-d_{10} after separation of biphenyl-d_{10}.

determined by ^{13}C NMR spectroscopy and by melting point. This would seem to indicate that these fragments were stable under these conditions and are probably not responsible for the initiation of this curing reaction in nitrogen, but rather might be a byproduct formed during the curing reaction. This is also supported by the fact that these products are not observed until essentially all of the resonances due to the phenylethynyl group, are over. This is shown in Fig. 24 by the ^{13}C NMR spectrum of a sample cured at 375°C for 30 min. The region from $\delta_C = 10$–50 ppm does not show any of these aliphatic carbon resonances. A possible conclusion for these results is that the phenylethynyl moiety is decomposing to possibly forming radicals that either add to (I) or couple with another radical to form dimers and subsequently form higher molecular weight material. When the concentration of (I) decreases to very low values, radical abstraction of an aromatic hydrogen becomes more favorable.

Since some fragments of model compound (I) are formed and also the MALDI-TOF MS (Fig. 6) indicates that much of the higher molecular weight material is 86–91 *m/z* different from the monomer (506 *m/z*), dimer (918 *m/z*) and trimer (1155 and 1331 *m/z*), these masses may correspond to a benzyl fragment. This may indicate that one part of the reaction may involve fragmentation of model compound at the triple bond. In order to investigate this possibility, some elemental analysis was performed in order to see if the cured material had the same empirical formula as the model compound (I). If fragmentation of the triple bond was occurring, perhaps some of the model compound may have been lost as volatile products. These results are shown in Table 4. There does not appear to be a great difference in these ratios. For instance, if the curing reaction involved fragmentation of the triple bond to produce some sort of benzyl fragment, some of the ratios might be different as the benzyl fragment is about 95% carbon by weight. Also, if this was the case, 1,2-diphenylethane should be observed in the various mass spectra of the cured products (Fig. 18), which it is not so. GC–MS experiments were also performed on the head gas of a cured sample and conclusions could not be made that curing involved fragmentation of the phenylethynyl group and possibly a loss of a low molecular weight volatile.

In addition to using model compound (I) for these thermal

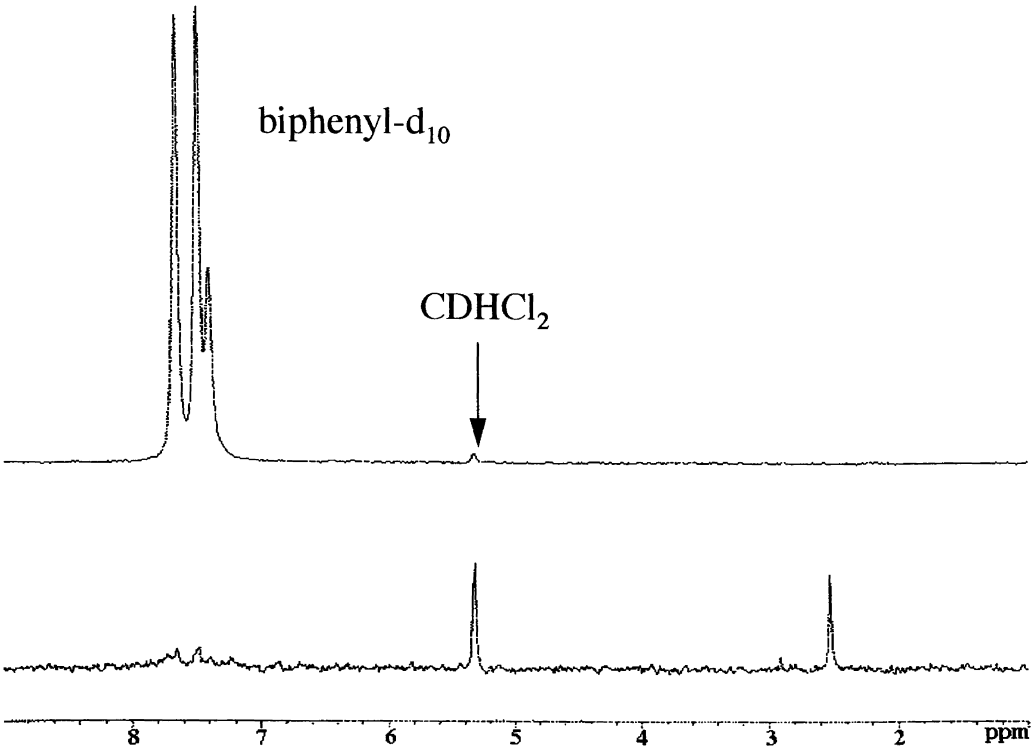

Fig. 22. ^{2}H NMR spectra of biphenyl-d_{10} and (I) cured at 375°C for 3 h with biphenyl-d_{10} after separation.

Table 3
Relative abundances of isotopes determined by EI mass spectrometry

Peak mass (*m*/*z*)	329	330	331	419	420	421
Theoretical	100	23.5	3.23	100	31.17	5.29
Fragment (II)	100	23.1	2.64			
Fragment (III)				100	31.1	5.4
Cured (I)[a]	100	23.7	3.9	100	31.0	5.2
Cured (I) w/deuterated biphenyl[b]	100	32.8	[c]	100	40.9	[c]

[a] 1 h cure.
[b] 3 h cure.
[c] Not reported due to low concentration.

Table 4
Elemental analysis of (I) and cured material

	% C	% H	% N	% O
Theoretical	80.95	4.12	3.37	11.56
Model compound (I)	80.92	4.14	3.23	11.71
(I) Cured in air[a]	79.79	4.10	3.23	9.93
(I) Cured in nitrogen[a]	78.75	4.04	3.20	10.79

[a] Samples cured for 1 h at 375°C.

Table 5
Influence of atmosphere on apparent first-order rate constants from data (derived from quantitative ^{13}C NMR experiments)

	Vacuum	Air	Oxygen
Apparent first-order rate constant (s^{-1})	2.5×10^{-4}	2.1×10^{-4}	1.3×10^{-4}
Correlation coefficient (R^2)	0.962	0.995	0.924

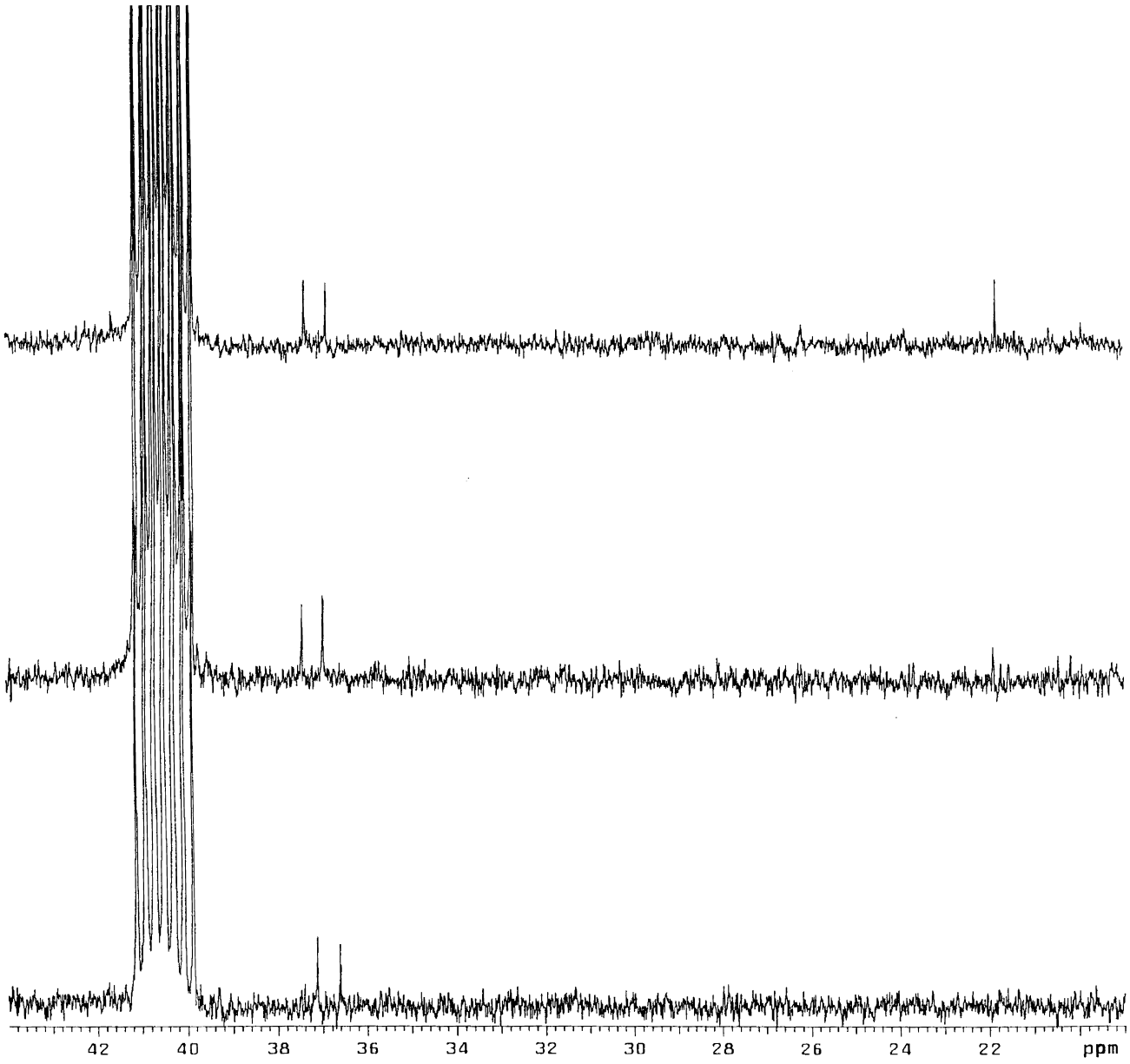

Fig. 23. ^{13}C NMR spectra of (I) cured for 1 h at 375°C (top), 4 h at 350°C (middle) and 9 h at 325°C (bottom).

Table 6
GPC data for the four samples cured under vacuum at 325°C

Cure time (h)	% Conversion	Total M_n (g mol^{-1})[a]	M_n of oligomer (g mol^{-1})[b]
1	75	630	1150
2	86	750	1180
3	95.6	970	1280
4	96.9	1100	1210

[a] Number average molecular weight of entire sample.
[b] Number average molecular weight of higher molecular weight fraction.

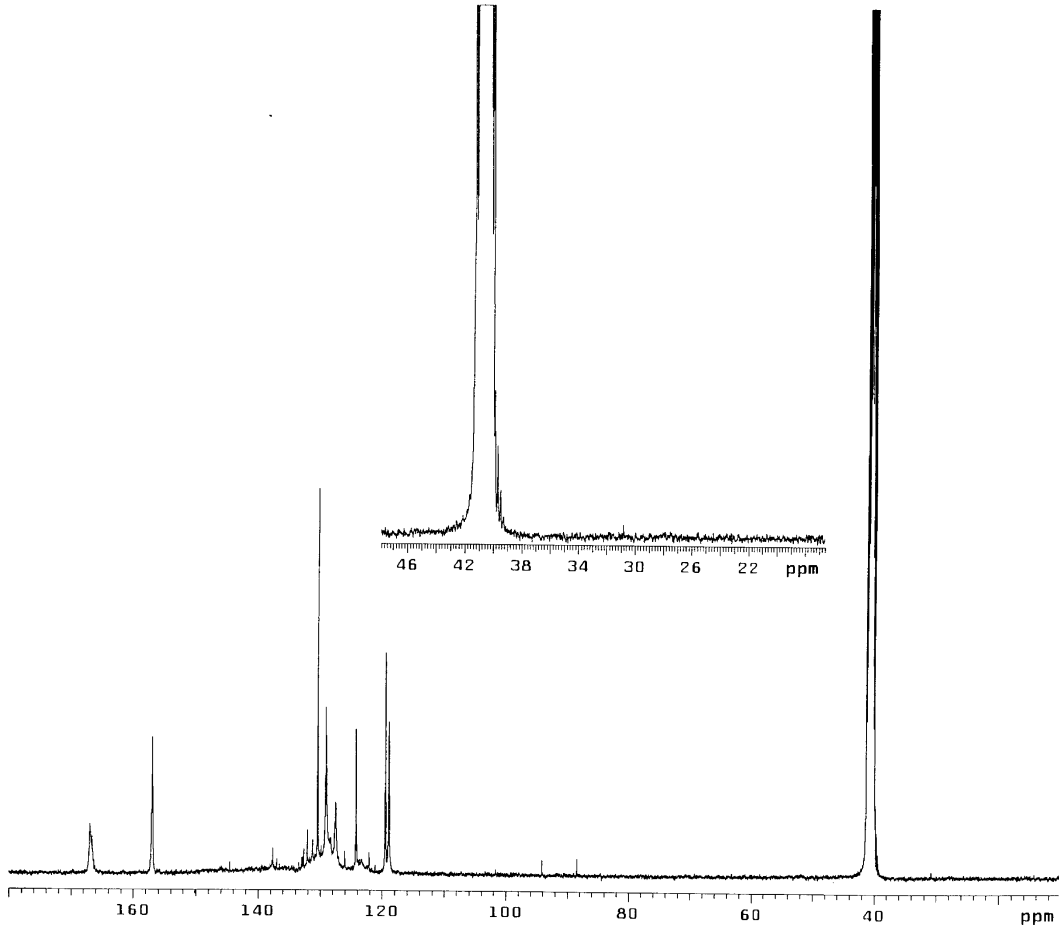

Fig. 24. ^{13}C NMR spectrum of (I) cured for 30 min at 375°C.

reactions, diphenylacetylene was cured at 325°C for 5 h under nitrogen. The ^{13}C NMR spectra of diphenylacetylene and the "cured" soluble diphenylacetylene are shown in Fig. 25. The spectrum of diphenylacetylene shows three peaks due to aromatic carbons and the phenylethynyl resonance at $\delta_C = 90$ ppm. The bottom spectrum shows the cured material. A variety of different resonances and peak broadening in the aromatic carbon region similar to cured samples of (I) is observed. Also, additional resonances in the aliphatic carbon region are present. The cure reaction did not go to completion as indicated by the presence of the phenylethynyl resonance at $\delta_C = 90$ ppm. Under these cure conditions, (I) undergoes complete conversion, whereas diphenylacetylene did not. This indicates that the electronic

Table 7
Apparent first-order rate constants for the thermal treatment of model (compound (I) under various conditions)

Temperature (°C)	Apparent first-order rate constant $\times 10^4$ (s^{-1})	Condition
315	3.1	Bulk
325	3.8	Bulk
325	3.9	Bulk
325	4.3	Bulk
325	4.7	Co-cure with 12% fragment (III)
325	3.3	Co-cure with 12% fragment (III)
325	4.8	Co-cure with 30 mol% $CuCl_2$
325	4.5	Co-cure with 30 mol% $CuCl_2$
335	16	Bulk
335	11	Bulk

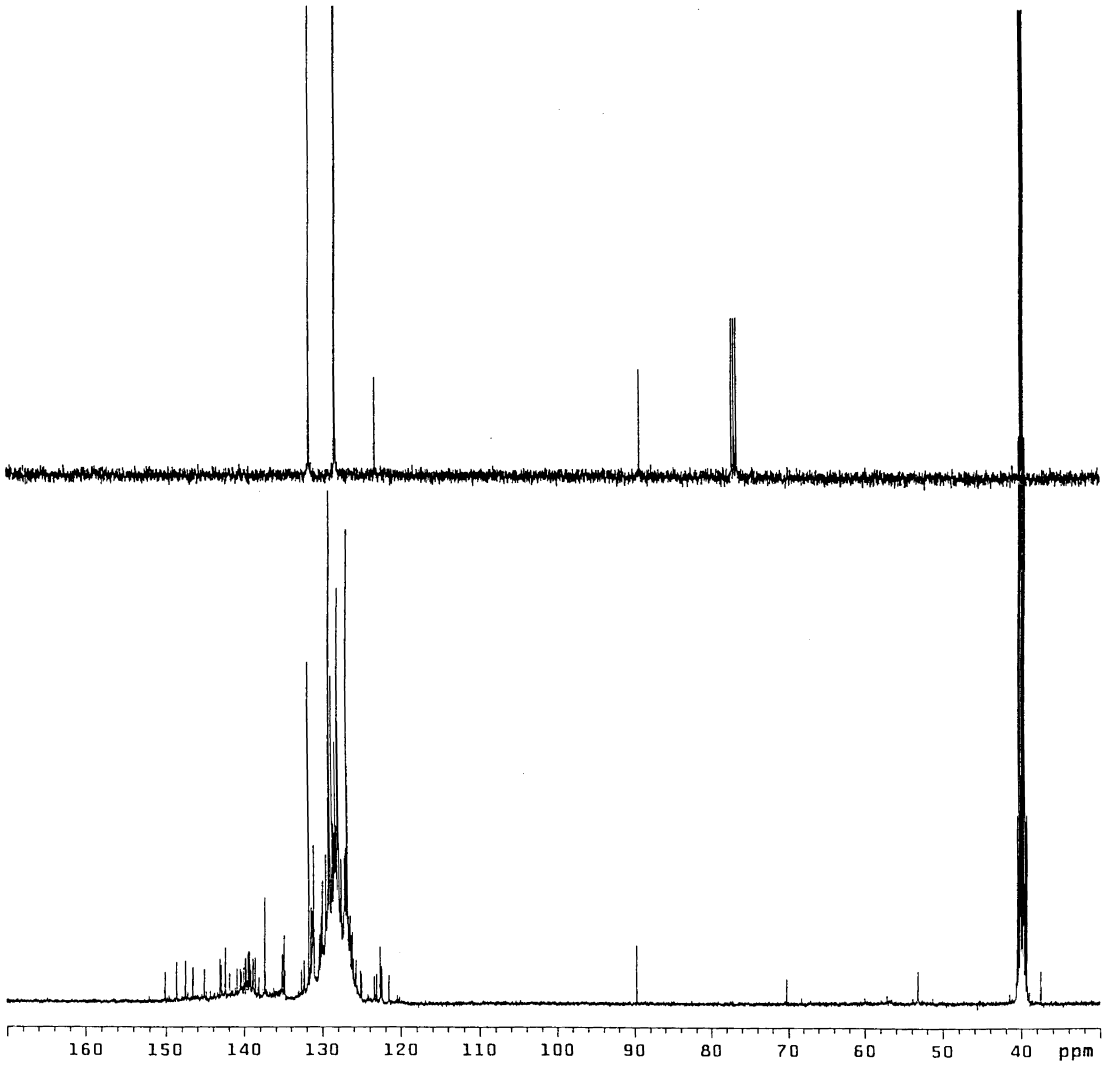

Fig. 25. ^{13}C NMR spectrum of diphenylacetylene (top) and diphenylacetylene "Cured" for 5 h at 325°C (bottom).

environment around the carbon–carbon triple bond affects at least the curing rate, if not the distribution of products. This has been demonstrated recently in our laboratory by Ayambem et al. [29]. GPC and mass spectral data indicates that higher molecular weight material is being formed up to about the pentamer. Additional low molecular peaks are evident in the mass spectrum including diphenylacetylene (178 *m*/*z*). Some of these low molar mass peaks could be due to similar structures as the ones found in the samples of cured (I).

The higher molecular weight fraction D was also investigated for possible structure(s) of the oligomeric material. The ^{13}C NMR spectrum of the fourth fraction (D) (Fig. 26) shows similar resonances to the crude cured product shown in Fig. 4, without some of the sharp resonances which are indicative of low molecular weight material. Fig. 26 indicates mainly broad resonances due to oligomeric material in the range of $\delta_C = 118$–170 ppm. The broad resonances are assigned to the carbon atoms 15–28 of (I) found in Table 1. Apparently, almost all of the resonances due to the phenylethynyl portion (carbon atoms 1–14) are either overlapping the diphenyl ether half, or are so broad that they are difficult to observe. Resonances becoming increasingly broad as the carbon atoms lose mobility is a common occurrence. The fact that the resonances of the phenylethynyl half of (I) are apparently very broad would seem to indicate that the oligomers are attached through the phenylethynyl group. One possible structure that has been suggested for the oligomeric material is a polyene type structure formed through the carbon–carbon triple bond. Empirical chemical shift results indicated that the conjugated polyene backbone carbons would appear at about $\delta_C = 140 \pm 6$ ppm. The inset in Fig. 26 shows a number of very broad resonances in this region that could be due to the polyene type structure for the oligomeric material, although definite further evidence of such a structure could not be found. Also, additional 2D NMR experiments could not be done due to the broad nature of the peaks of interest.

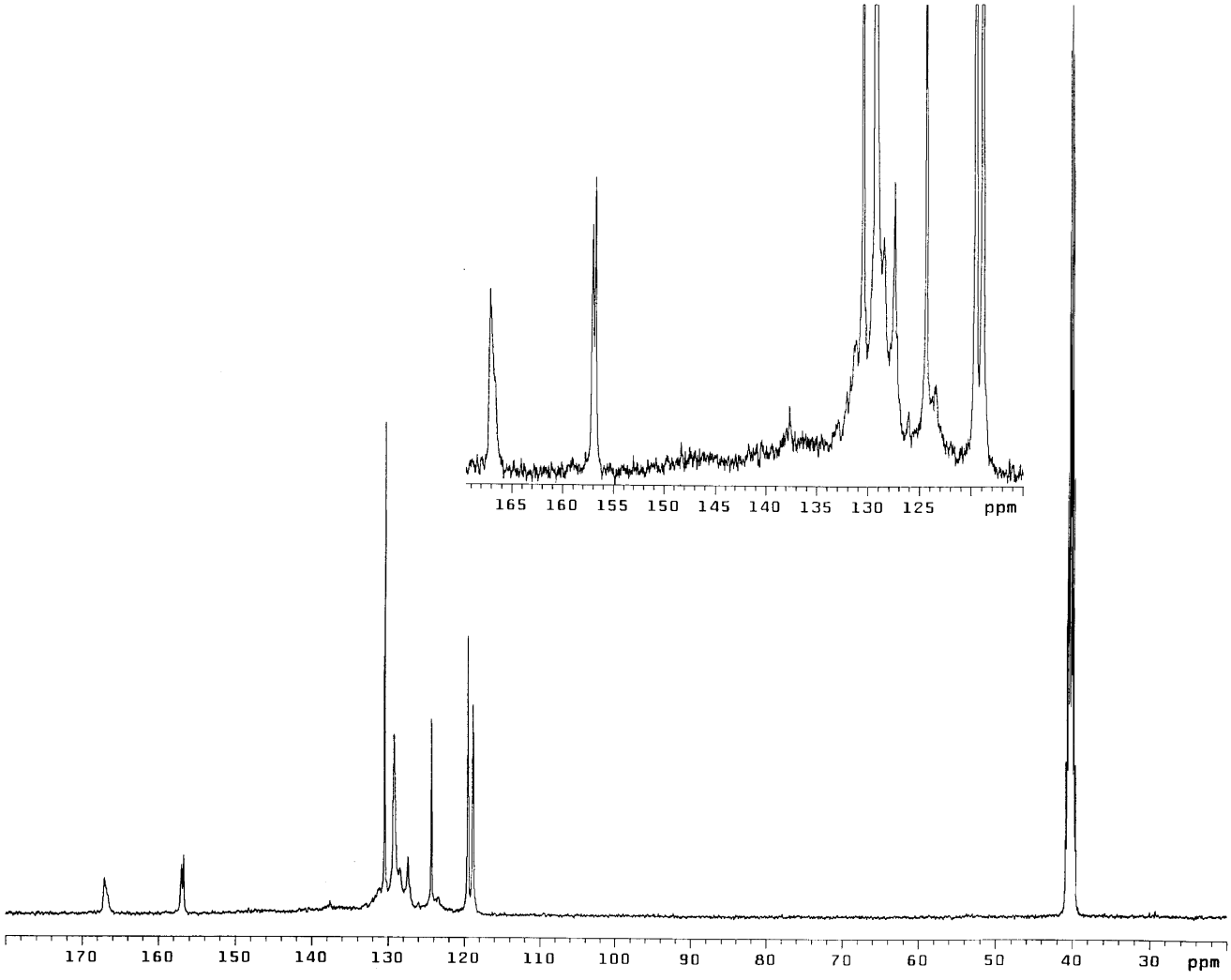

Fig. 26. ^{13}C NMR spectrum of the fourth fraction (D).

3.2. Kinetics

3.2.1. ^{13}C NMR

The kinetics of the curing reaction of model compound (I) was followed by the quantitative ^{13}C NMR and also FT-IR. For the quantitative ^{13}C NMR experiments, four samples of model compound (I) were thermally treated at 325°C for 1, 2, 3 and 4 h under vacuum, air and oxygen atmospheres. The amount of residual model compound was determined by integration of the two phenylethynyl resonances and comparing them to the integration of other resonances.

Fig. 27 shows the data plotted as $\ln(C_0/C)$ versus time, where C_0 and C are the concentrations of the phenylethynyl moiety at time 0 and time t, respectively. The slopes of these curves are the apparent first-order rate constants. This data is shown in Table 5 along with the correlation coefficients (R^2).

The plot shown in Fig. 27 and the data from Table 5 indicate that the rate is slower in pure oxygen compared to air or vacuum. One might expect that the rate would be lower in the presence of oxygen for a free radical reaction, although it is certainly possible that oxy radicals can initiate at these high temperatures [30].

The GPC traces of the samples cured under vacuum are shown in Fig. 28. A reduction of the peak due to the model compound at a retention volume of about 28 ml decreases as the cure time is increased. Also, high molecular weight products are being formed early in the reaction, which is characteristic of classical free radical addition polymerization kinetics. Table 6 shows the GPC data for the four samples cured under vacuum at 325°C. This table shows the molecular weight of each sample the conversion and the molecular weight of the oligomeric material (from 23 to 27.5 ml). The data from Table 6 indicate, as the total molecular weight increases with time, the molecular weight of the polymer formed remains almost the same.

3.2.2. FTIR

The kinetics of the thermal reaction of model compound (I) was also followed by FT-IR. The FT-IR spectrum of model compound (I) at 325°C was taken vs. time. A typical first-order plot of $\ln(C_0/C)$ vs. time is shown in Fig. 29. The

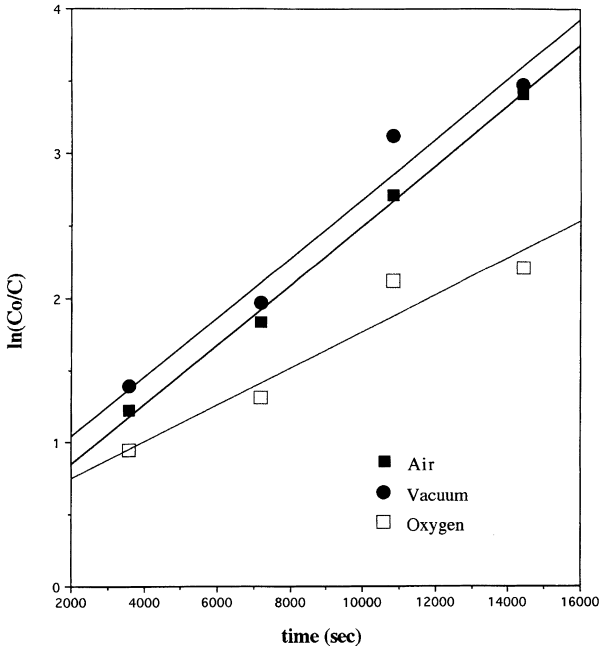

Fig. 27. First-order plots of (I) cured at 325°C in nitrogen as determined by ^{13}C NMR spectroscopy.

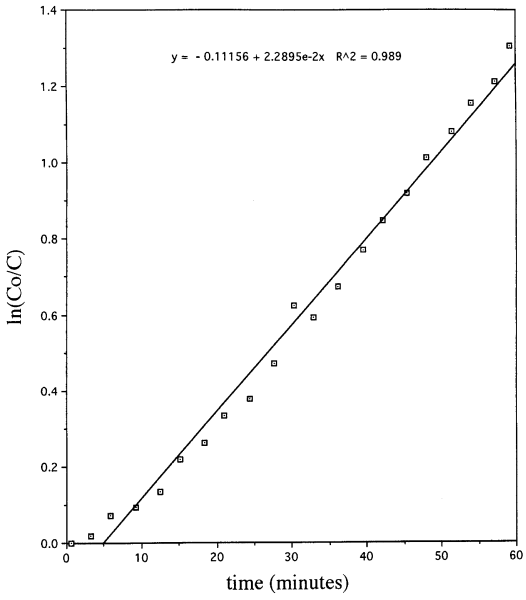

Fig. 29. First-order plots of (I) cured at 325°C under nitrogen as determined by FT-IR spectroscopy.

second-order plot of $1/(C)$ vs. time of the same data is shown in Fig. 30. The data points from Fig. 30 obviously vary from linearity more than those in Fig. 29. The reaction would appear to be first order as determined by both FT-IR and by quantitative ^{13}C NMR experiments throughout the reaction. In addition to curing only the model compound (I) under these conditions, experiments were also performed in the presence of fragment (III) or $CuCl_2$ and at 315 and 335°C. All of the apparent first-order rate constants of all these reactions are shown in Table 7. The addition of fragment (III) or the copper salt did not appear to change the rate of disappearance of the phenylethynyl group. This would also seem to indicate that this fragment is not involved in the initiation or propagation reactions.

4. Conclusions

Thermal curing of the crystalline model compound (I) produces amorphous ($T_g > 200$°C) oligomeric products of higher molecular weight and also low molecular weight fragments. Thermal treatment at 375°C for 1 h under nitro-

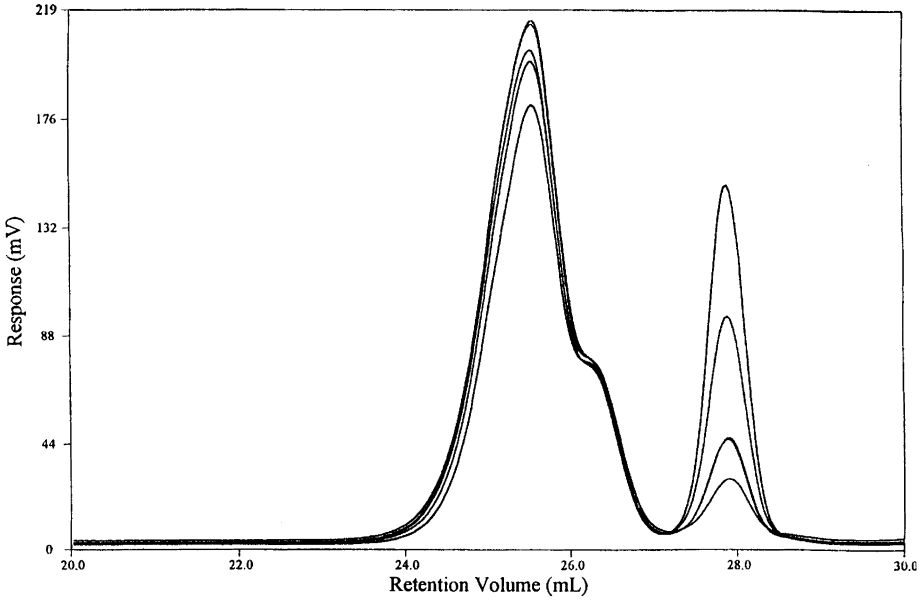

Fig. 28. GPC traces in chloroform of (I) Cured at 325°C.

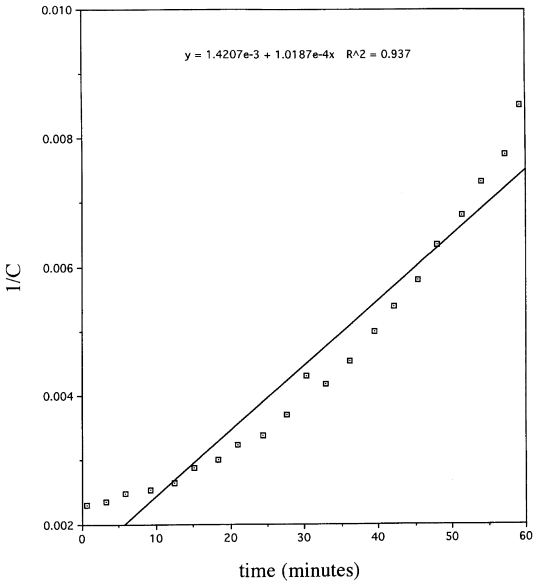

Fig. 30. Second-order plot of (I) cured at 325°C under nitrogen determined by FT-IR spectroscopy.

gen produced a fully "cured" model compound as determined by ^{13}C NMR spectrometry, which was still readily soluble. This result indicates that the single phenylethynyl moiety is difunctional. The structure of the higher molecular weight material is as yet poorly characterized because of line broadening. A number of fragments were produced, and their type and concentration were dependent on the curing temperature and appear to be generated only after essentially complete conversion of the phenylethynyl group. Interestingly, these fragments contained aliphatic protons that were not present in the model compound. These protons were postulated to originate from aromatic protons since they were the only ones present. Co-curing studies using biphenyl-d_{10} and model compound (I) produced scrambling of the deuterium atoms, to specifically the methyl group of fragment (II) and possibly also the methylene carbon of fragment (III). This would seem to indicate that the reactive intermediate generated with the thermal treatment of (I) is able to abstract aromatic deuterium atoms from biphenyl-d_{10}. The thermal curing reaction was determined to follow first-order kinetics as determined by FT-IR and ^{13}C NMR. The rate of reaction slows as the concentration of oxygen increases.

Acknowledgements

The author would like to thank the National Science Foundation and Technology Center for support under contract DMR-9120004. Washington University Mass Spectrometry Resource, an NIH Research Resource (Grant No. P41RR0954) for the MALDI-TOF MS experiments, Dr Qing Ji for the GPC experiments and Kim Harich for the EI mass spectrometry experiments.

References

[1] Jensen BJ, Hergenrother PM, Nwokogu G. Polyimides with pendent ethynyl groups. Polymer 1993;34:630.
[2] Jensen BJ, Hergenrother PM, Nwokogu G. Poly(arylene ethers) with pendent ethynyl groups. J Macromol Sci, Pure Appl Chem A 1993;30(6/7):449.
[3] Harrington KA, Orwoll RA, Jensen BJ, Young PR. Characterization of cure chemistry of selected phenylethynyl-terminated polyimides and model compounds. Society of Advanced Materials and Process Engineering Series 1996;41:135.
[4] Cooper JB, Wise KL, Jensen BJ. Modulated FT-Raman fiber-optic spectroscopy: a novel technique for remotely monitoring high temperature reactions in real-time. Anal Chem 1997;69(11):1973.
[5] Tan B, Tchatchoua CN, Vasudevan V, Dong L, McGrath JE. Polym Adv Tech 1997;9:84–93.
[6] Hergenrother PM, Bryant RG, Jensen BJ, Havens SJ. J. Polym Sci, Polym Chem Ed 1994;32:3061.
[7] Johnston JA, Li FM, Harris FW, Takekoshi T. Polymer 1994;35:4865.
[8] Yang Hi, Hay AS. J Macromol Sci, Pure Appl Chem A 1994;31(2):155.
[9] Smith JG, Connell JW, Hergenrother P, Gardner S. Polymer 1997;18:4657.
[10] Takeichi T, Tanikawa M. J Polym Sci, Part A: Polym Chem 1996;34:2205.
[11] Mecham SJ. PhD dissertation, Virginia Polytechnic Institute and State University, 1997.
[12] Joseph WD, Abed JC, Yoon TH, McGrath JE. Polym Prepr Am Chem Soc Div Polym Chem 1994;35(1):551.
[13] Joseph WD. PhD dissertation, Virginia Polytechnic Institute and State University, 1994.
[14] Jensen JJ, Mathias LJ. Polym Prepr. Am Chem Soc Div Polym Chem 1997;38(1):180.
[15] Hinkley JA, Jensen BJ. High Perform Polym 1996;8:599.
[16] Sefcik MD, Stejskal EO, McKay RA, Schaefer J. Macromolecules 1979;12:423.
[17] Ratto JJ, Dynes PJ, Hamermesh LL. J Polym Sci, Polym Chem 1980;18:1035.
[18] Swanson SA, Fleming WW, Hofer DC. Macromolecules 1992;25:582.
[19] Kovar RF, Ehlers GFL, Arnold FE. J Polym Sci, Polym Chem 1977;15:1081.
[20] Pickard JM, Jones EG, Goldfarb IJ. Macromolecules 1979;12:895.
[21] Gandon S, Mison P, Sillion B. Polymer 1994;38:1449.
[22] Takekoshi T, Terry JM. Polymer 1994;35:4874.
[23] Meyer GW, Glass TE, Grubbs HJ, McGrath JE. J Polym Sci Polym Chem Div Polym Chem 1995;33:2141.
[24] Wood KH, Ovwoll RA, Jensen BJ, Young PR, McNair HM. Polym Prepr Am Chem Soc Div Polym Chem 1997;38(1):266.
[25] Tan B. PhD dissertation, Virginia Polytechnic Institute and State University, 1997.
[26] Bax A, Summers MF. J Am Chem Soc 1986;108:2093.
[27] Harwood HJ, Russell DB, Verthe JJA. Zymonas. Makromol Chem 1973;163:1.
[28] Mango LA, Lenz RW. Makromol Chem 1973;163:13.
[29] March J. Advanced organic chemistry, 4th. , 1992. pp. 226–230.
[30] Ayambem A, Mecham S, McGrath JE. Polym Prepr Am Chem Soc Div Polym Chem 1997;38(2):373.
[31] Meyer GW, Heidbrink JL, Franchina JG, Davis RM, Gardner S, Vasudevan V, Glass TE, McGrath JE. Polymer 1996;37:5077.